iP2i
LES 2 INFINIS
LYON

Journey to the center of...

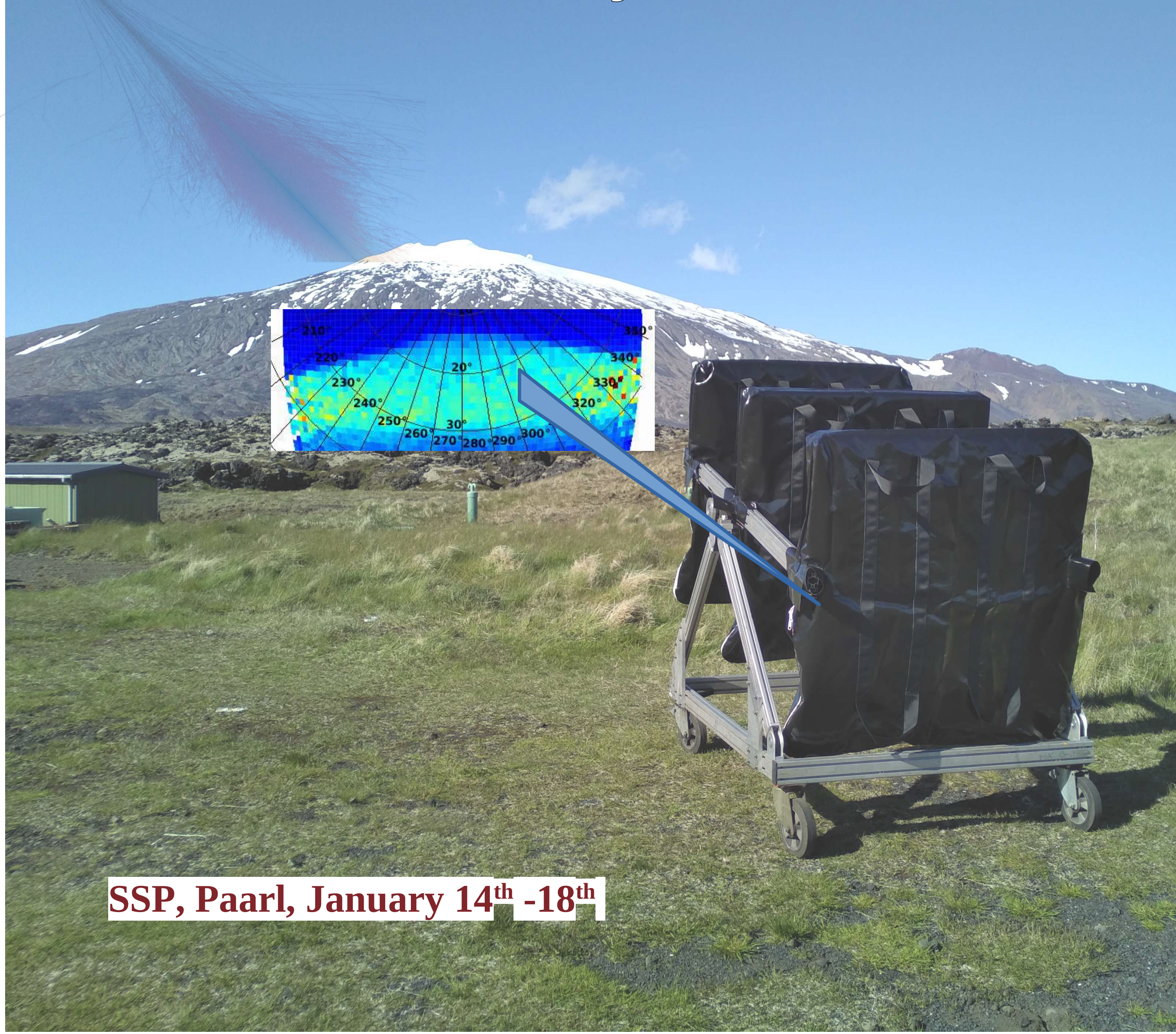

SSP, Paarl, January 14th -18th

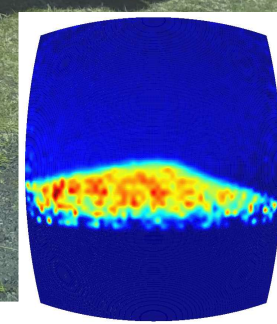

cnrs
IN2P3
Les deux infinis

UCBL Lyon 1

Muography general features

$$\left\langle -\frac{dE}{dx}\right\rangle = Kz^2\frac{Z}{A}\frac{1}{\beta^2}\left[\frac{1}{2}\ln\frac{2m_ec^2\beta^2\gamma^2W_{\max}}{I^2} - \beta^2 - \frac{\delta(\beta\gamma)}{2}\right]$$

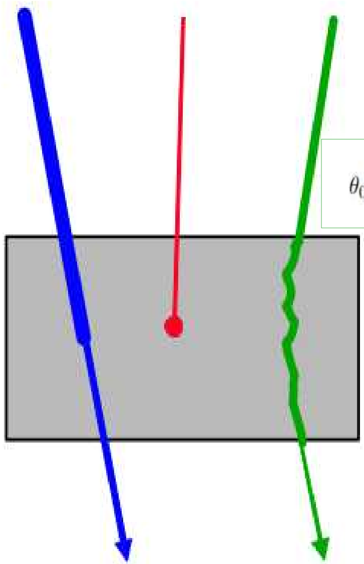

$$\theta_0 = \frac{13.6\ \mathrm{MeV}}{\beta cp}\, z\sqrt{\frac{x}{X_0}}\left[1+0.088\log_{10}\left(\frac{x z^2}{X_0\beta^2}\right)\right]$$

Different types of interaction between muons and matter: trajectories with and without scattering (green and blue lines), stopping trajectories (red line).

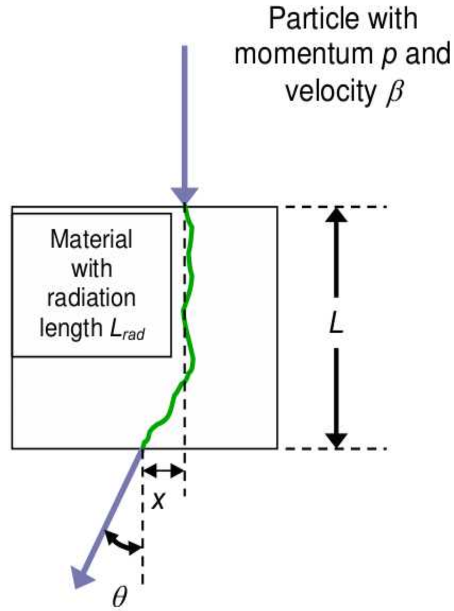

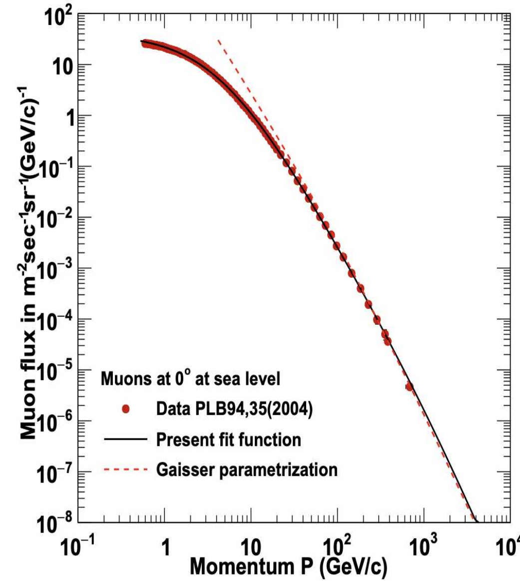

POCA 3D: Point of Closest-Approach

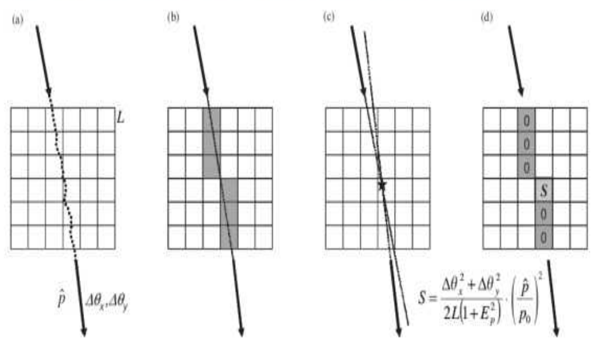

Fig. 4. PoCA reconstruction algorithm, shown in 2D for simplicity. A muon's stochastic path through an object volume (a). We measure scattering in two planes, and estimate particle momentum. Estimate muon path and identify voxels through which ray passed (b). Localize scattering signal to voxel containing PoCA (c). Define scattering signal as shown, and assign signal to the PoCA voxel, 0 to other candidate voxels (d). Take mean signal in each voxel over all muons to establish reconstructed scattering strength.

Pour chaque muon

I : Nombre de muons par cellule : Pour toute cellule collorée : ajoute 1

S : Scattering Influence : Pour toute cellule colorée : ajoute Score S

λ : Densité de Scattering : $\lambda(j) := S(j)/I(j)/L$

MLEM: Maximum Likelihood Expectation Maximisation

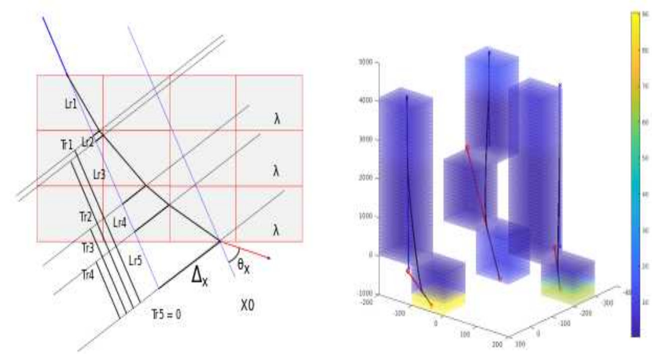

x

$$P(D_i|\lambda) = \frac{1}{2\pi|\Sigma_i|^{1/2}}\exp\left(-\frac{1}{2}D_i^T\Sigma_i^{-1}D_i\right).$$

y

$$P(D_i|\lambda) = \frac{1}{2\pi|\Sigma_i|^{1/2}}\exp\left(-\frac{1}{2}D_i^T\Sigma_i^{-1}D_i\right).$$

X

$$\frac{1}{|\Sigma|}\left(\Delta\theta_i^2 v_{w,i} - 2\Delta\theta_i w_i s_{\theta w,i} + \Delta w_i^2 v_{\theta,i}\right)$$

$$\Sigma_i = p_{r,i}^2\sum_{j\le N}\lambda_j W_{ij}.$$

$$W_{ij} \equiv \begin{bmatrix} L_{ij} & L_{ij}^2/2 + L_{ij}T_{ij} \\ L_{ij}^2/2 + L_{ij}T_{ij} & L_{ij}^3/3 + L_{ij}^2T_{ij} + L_{ij}T_{ij}^2 \end{bmatrix}$$

P (D/λ) Vraisemblance :
Probabilité que l'observable (Angle de diffusion + Déplacement) existe sachant la distribution de densité proposée

Muography use cases overview

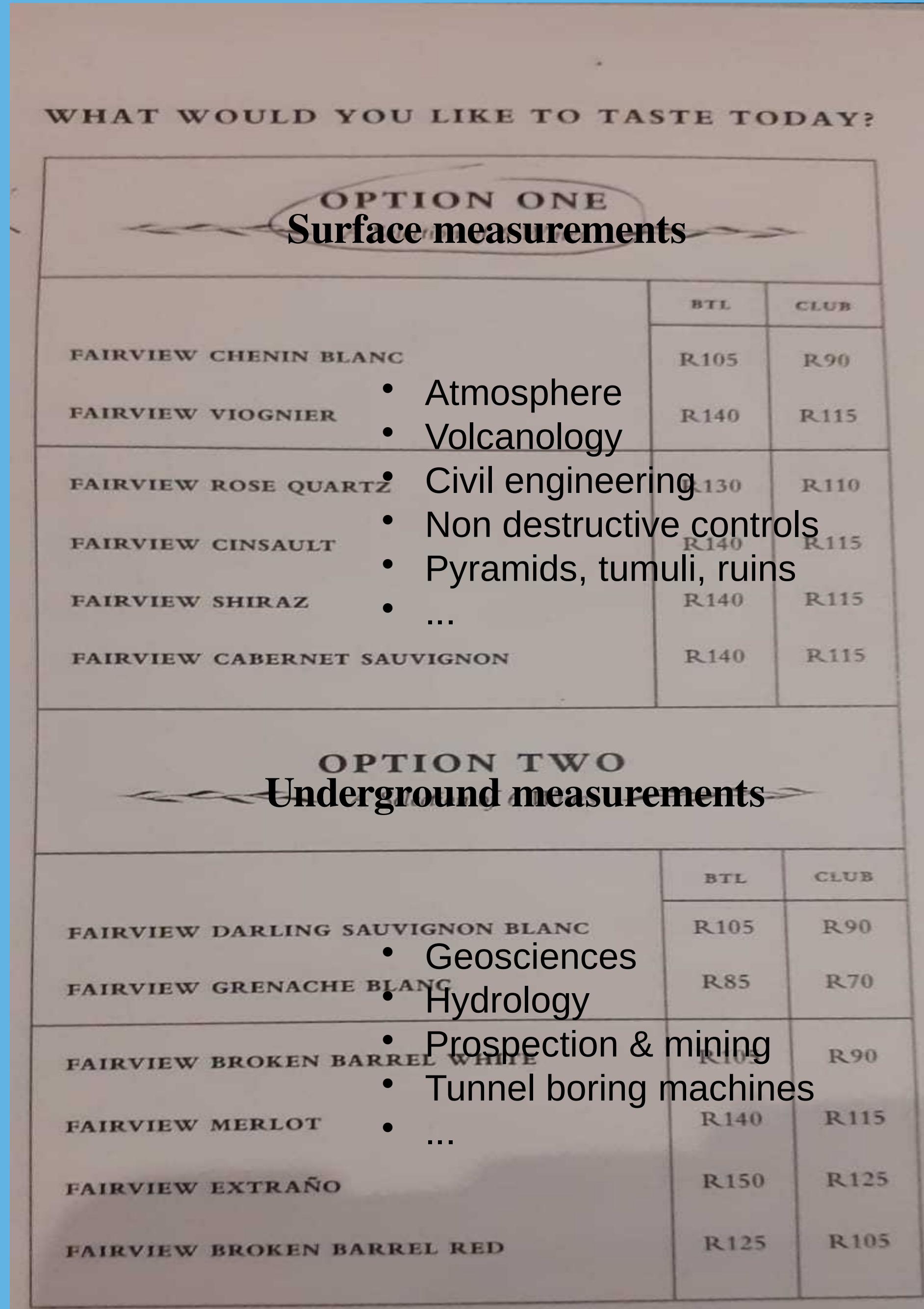

WHAT WOULD YOU LIKE TO TASTE TODAY?

OPTION ONE

	BTL	CLUB
FAIRVIEW CHENIN BLANC	R105	R90
FAIRVIEW VIOGNIER	R140	R115
FAIRVIEW ROSE QUARTZ	R130	R110
FAIRVIEW CINSAULT	R140	R115
FAIRVIEW SHIRAZ	R140	R115
FAIRVIEW CABERNET SAUVIGNON	R140	R115

OPTION TWO

	BTL	CLUB
FAIRVIEW DARLING SAUVIGNON BLANC	R105	R90
FAIRVIEW GRENACHE BLANC	R85	R70
FAIRVIEW BROKEN BARREL WHITE	[illegible]	R90
FAIRVIEW MERLOT	R140	R115
FAIRVIEW EXTRAÑO	R150	R125
FAIRVIEW BROKEN BARREL RED	R125	R105

Surface measurements

- Atmosphere
- Volcanology
- Civil engineering
- Non destructive controls
- Pyramids, tumuli, ruins
- ...

Underground measurements

- Geosciences
- Hydrology
- Prospection & mining
- Tunnel boring machines
- ...

Tracking

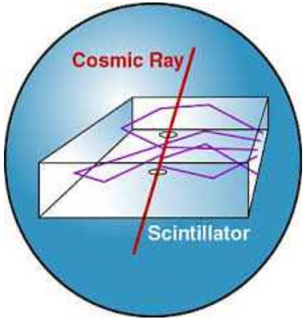

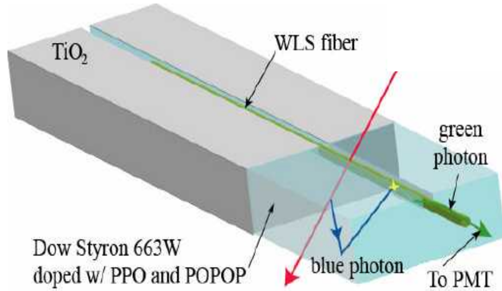

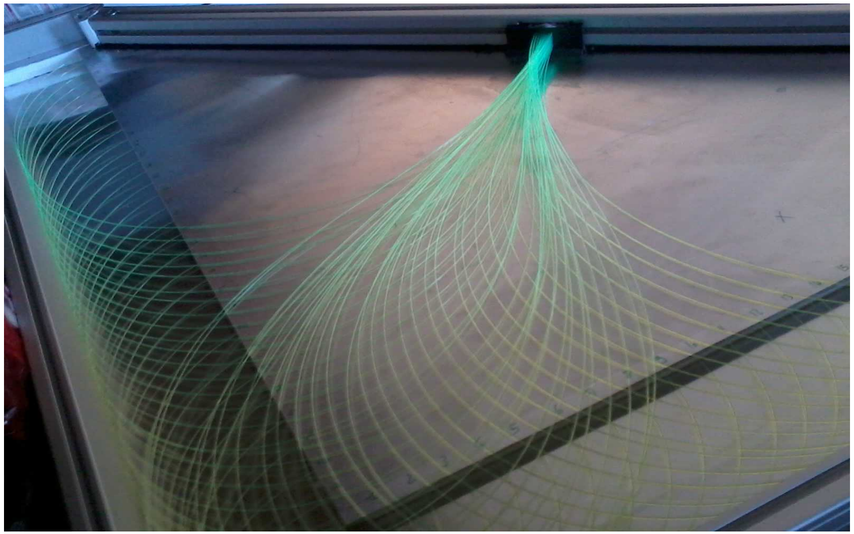

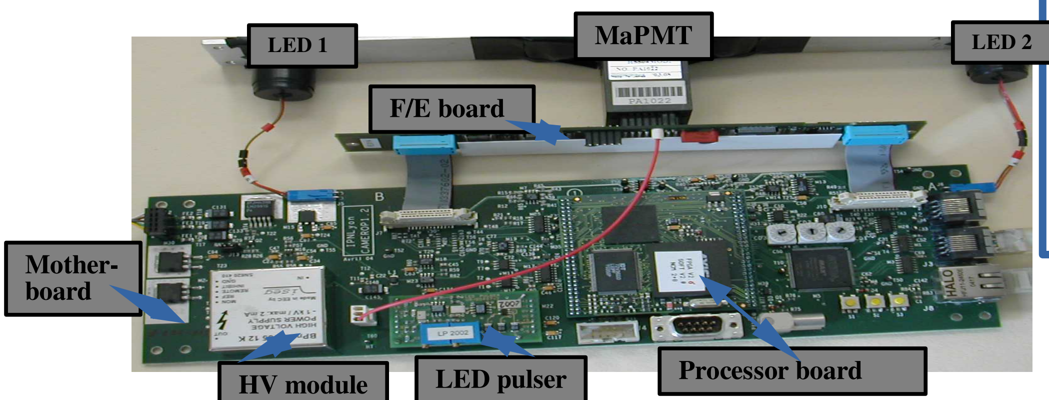

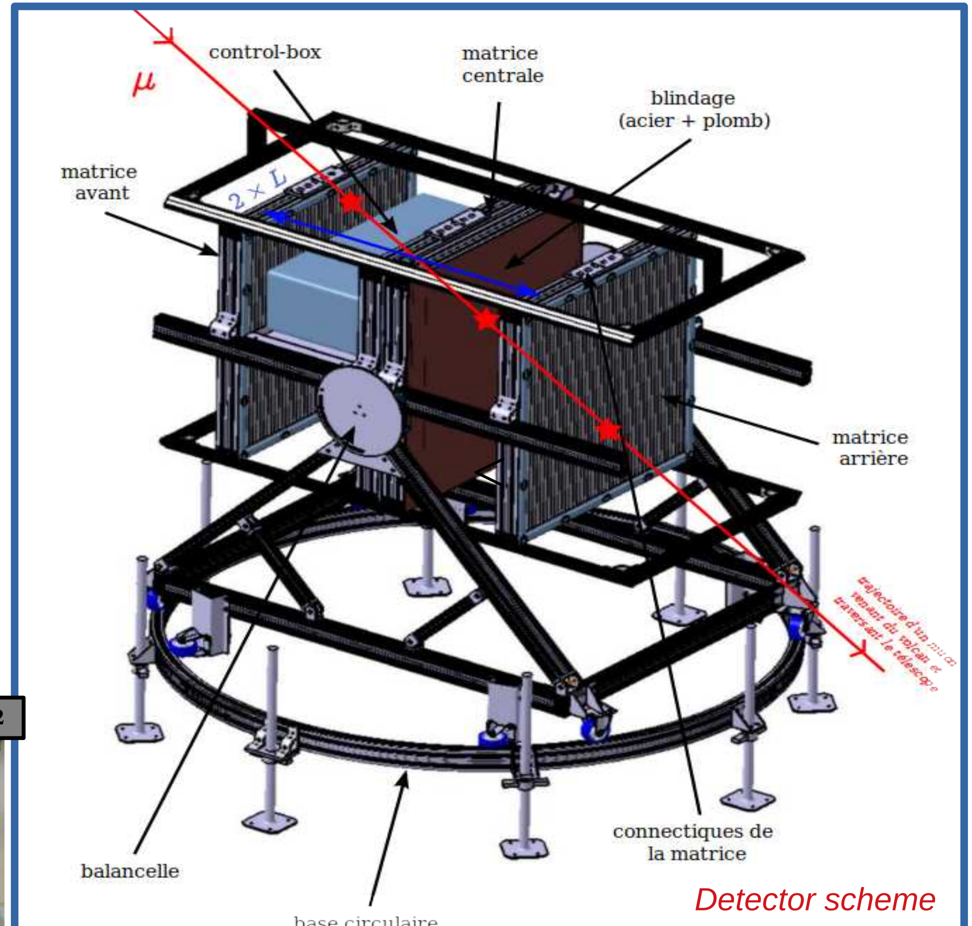

Detector scheme

Imaging **capabilities**

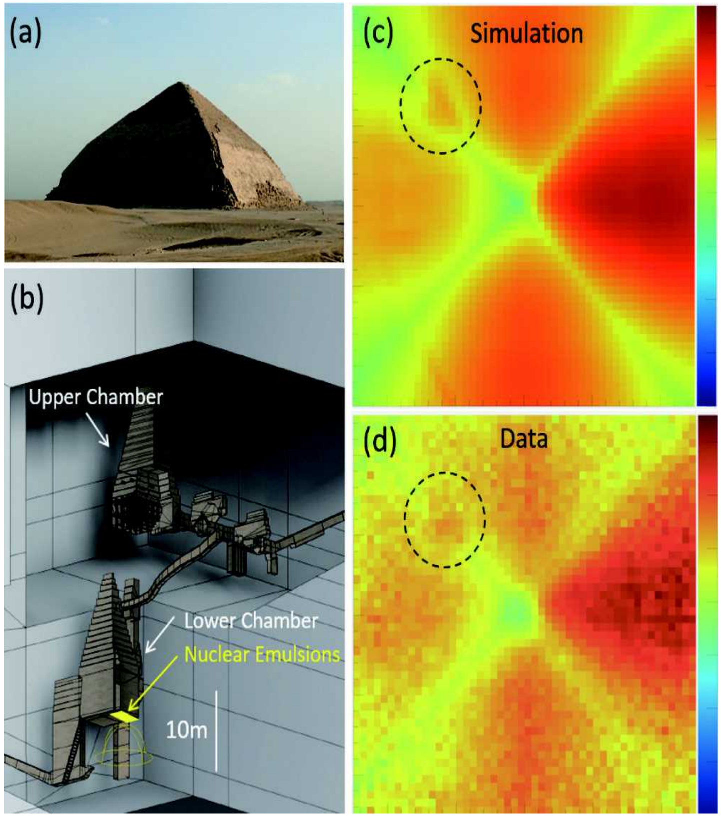

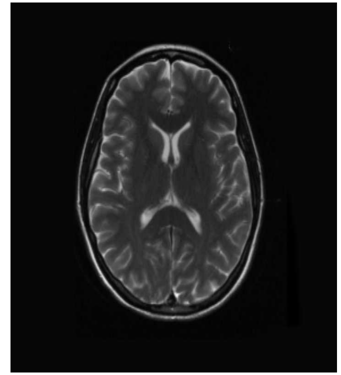

Detector → data

Reconstruction → inverse problem

Images

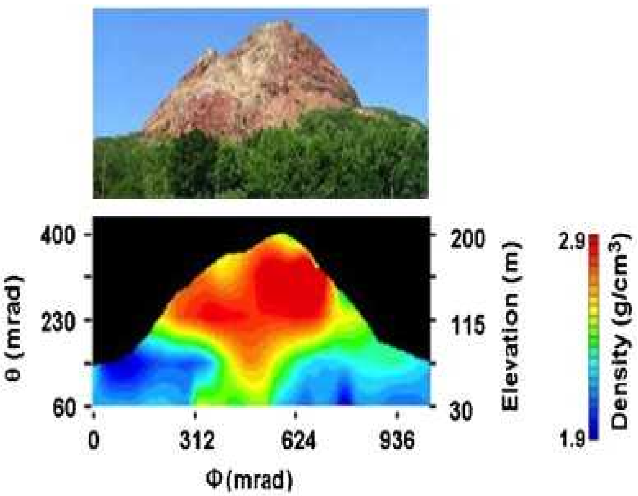

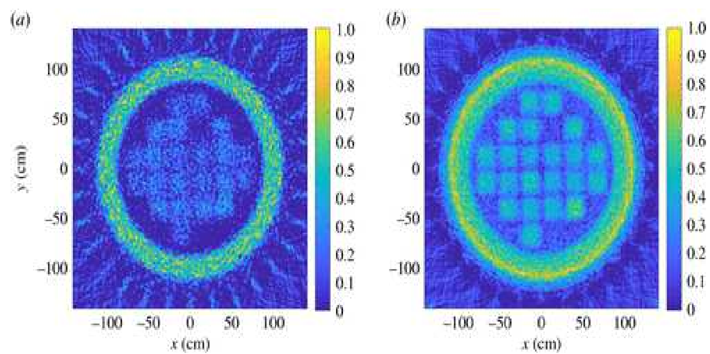

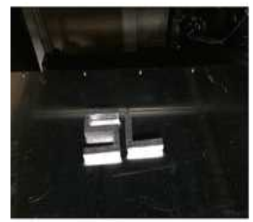

Images

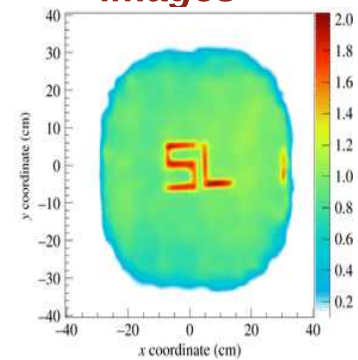

Monitoring capabilities – P & T sensitivity

Water level monitoring of a water tower tank

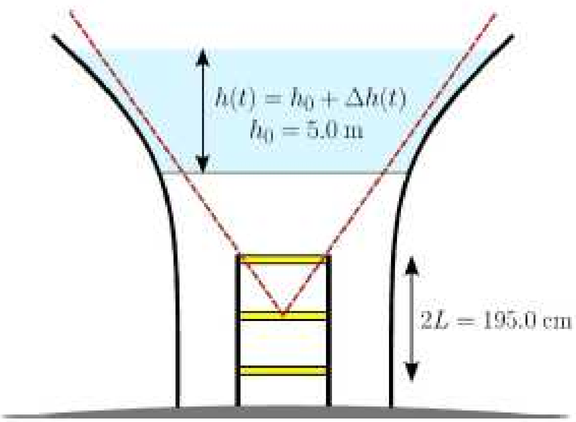

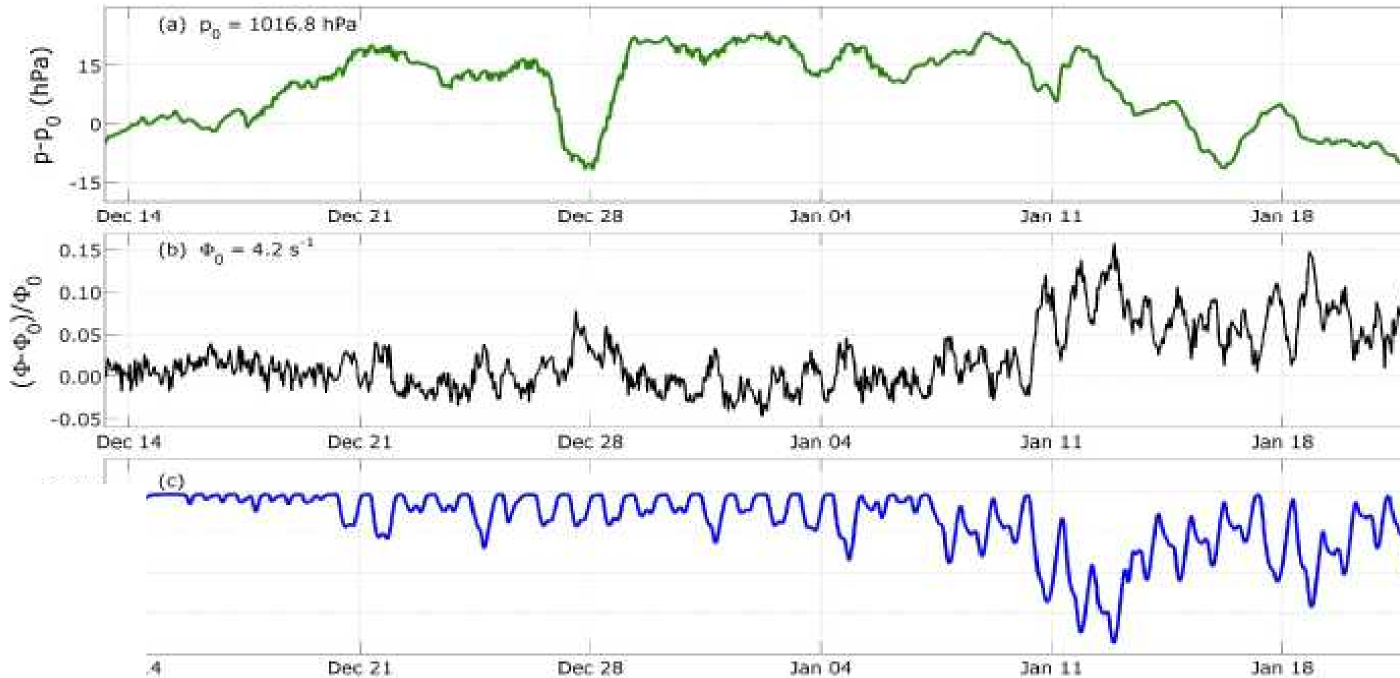

Low energy cut ~1.5 GeV:

- high statistics
- time resolution
- E-dependent barometric effects

$$\frac{\Delta R}{\langle R\rangle} = \alpha_T \frac{\Delta T_{\rm eff}}{\langle T_{\rm eff}\rangle} + \beta_P (p - \langle p\rangle)$$

- geomagnetic effects
- solar activity effects

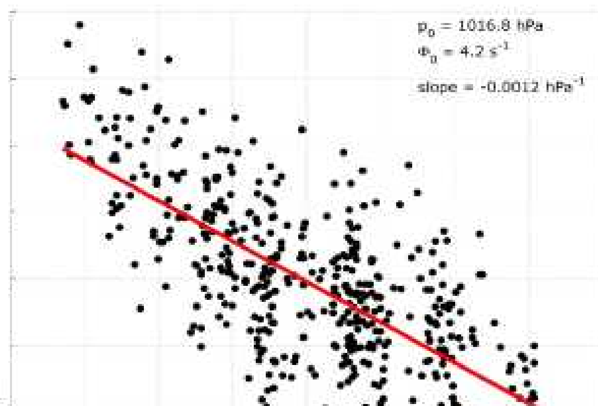

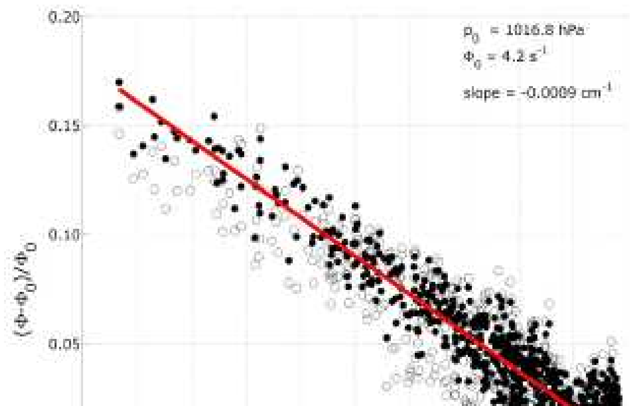

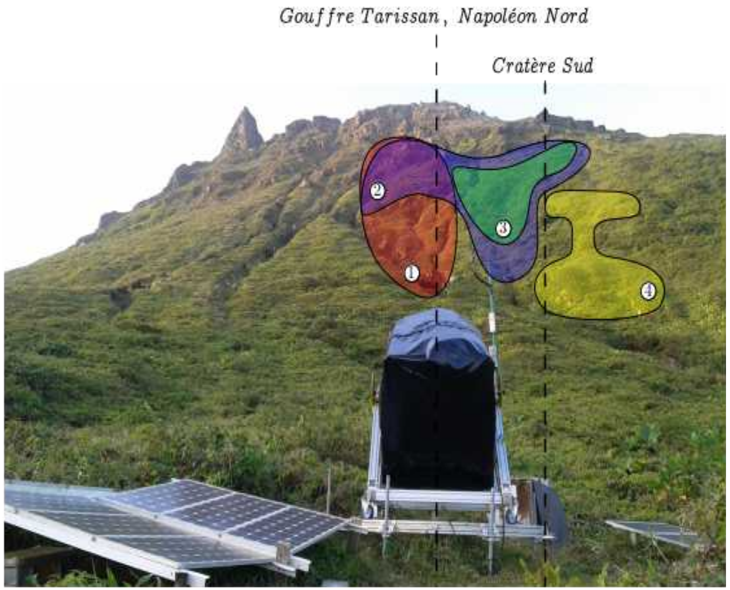

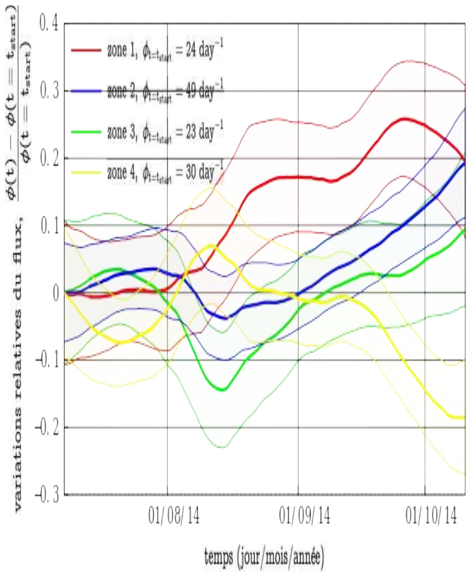

La Soufrière de Guadeloupe

Snaefellsjökull

Volcanoes

Etna

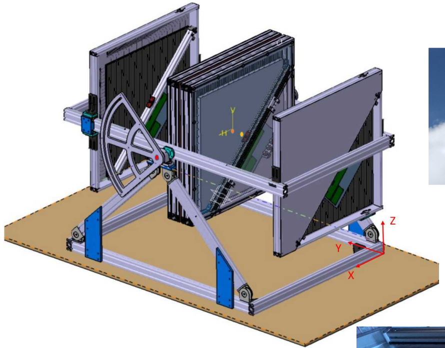

3-planes scintillator tracker
(author : J.-C.Ianigro).

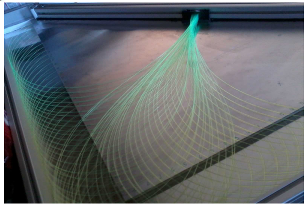

Mayon

Imaging & monitoring

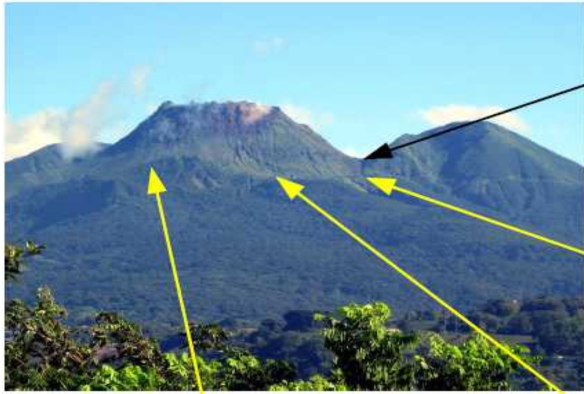

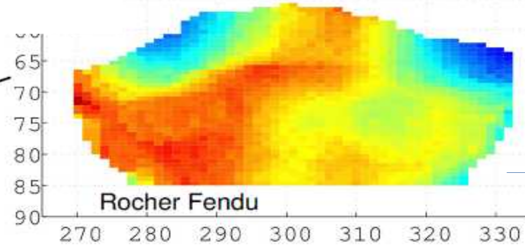

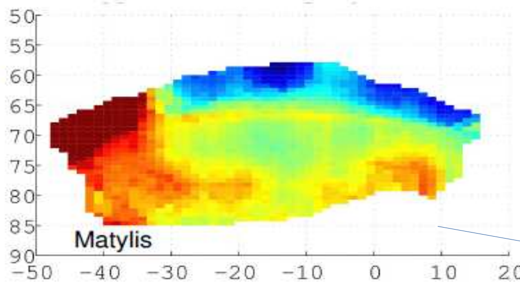

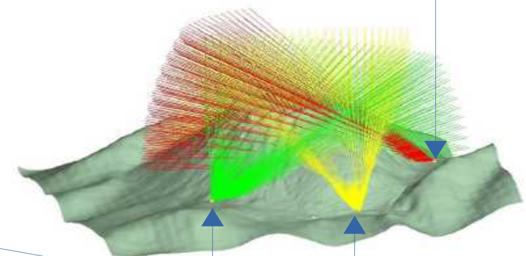

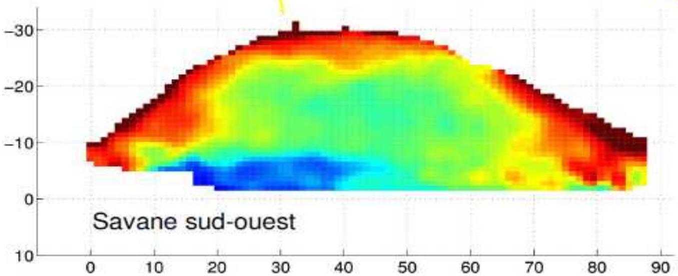

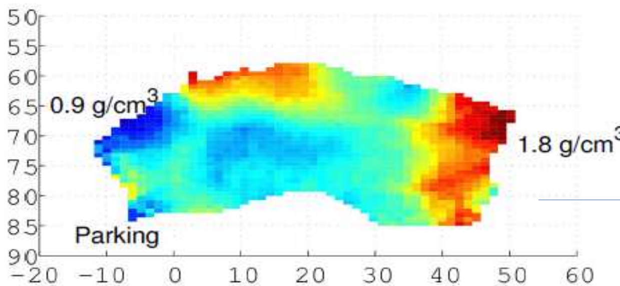

The largest muons station in the world (6 detectors running)

3-D gravi-muon joint inversion

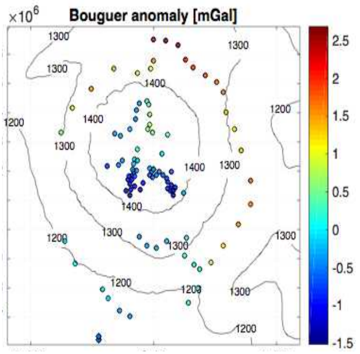

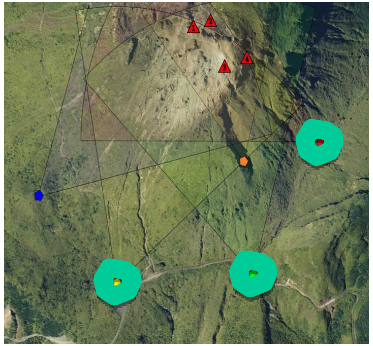

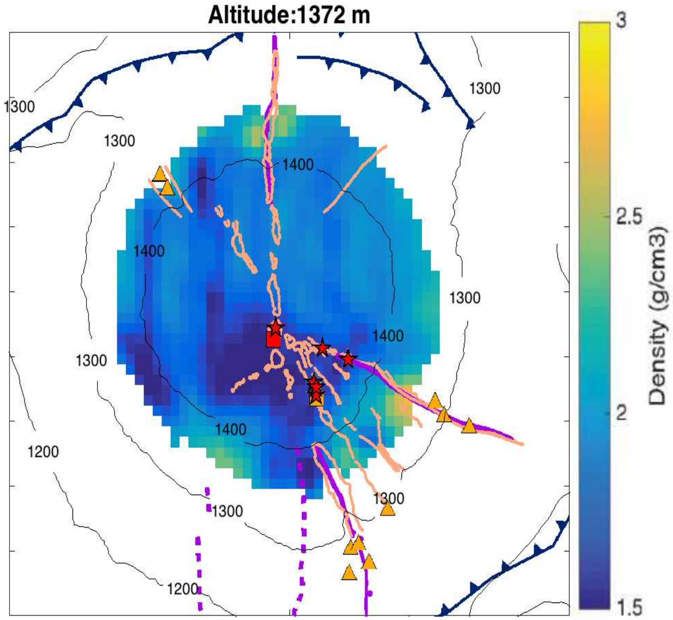

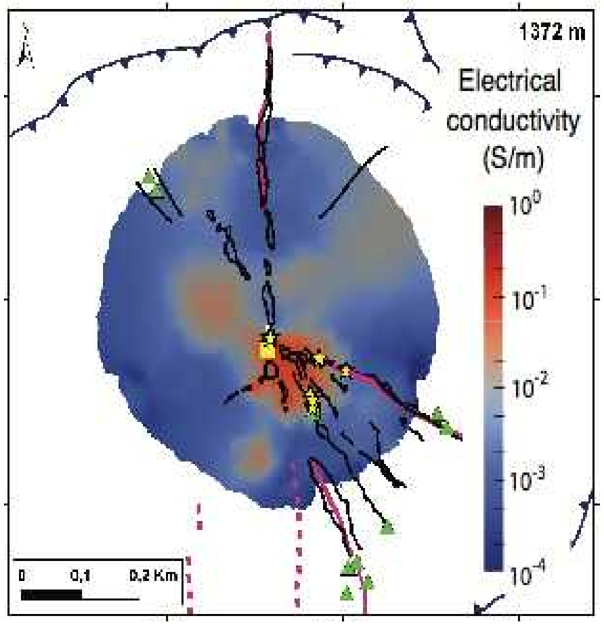

(Rosas-Carbajal et al., 2017)

$$G \begin{bmatrix} \boldsymbol{\rho}_\mu \\ \Delta\rho \end{bmatrix} = \begin{bmatrix} G_g \\ G_\mu \end{bmatrix} \begin{bmatrix} \boldsymbol{\rho}_\mu \\ \Delta\rho \end{bmatrix} = \begin{bmatrix} \mathbf{d}_g \\ \mathbf{d}_\mu \end{bmatrix} = \mathbf{d}$$

$$\phi(\mathbf{m}) = (\mathbf{d} - G\mathbf{m})^T C_d^{-1} (\mathbf{d} - G\mathbf{m}) + \\ + \epsilon^2 (\mathbf{m} - \mathbf{m}_{prior})^T C_\rho^{-1} (\mathbf{m} - \mathbf{m}_{prior}),$$

Smoothing

Damping

Matrix scaling

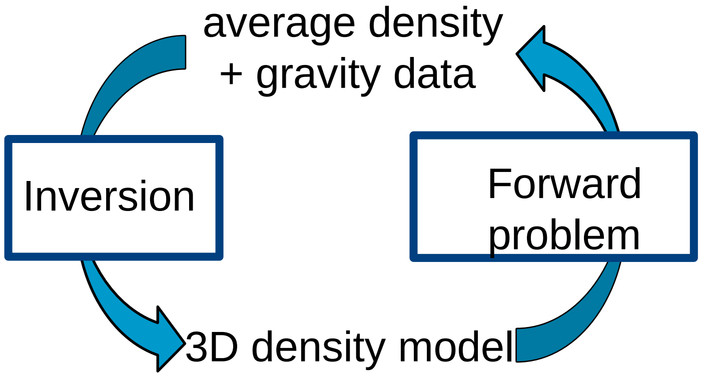

Sismo-muon joint monitoring

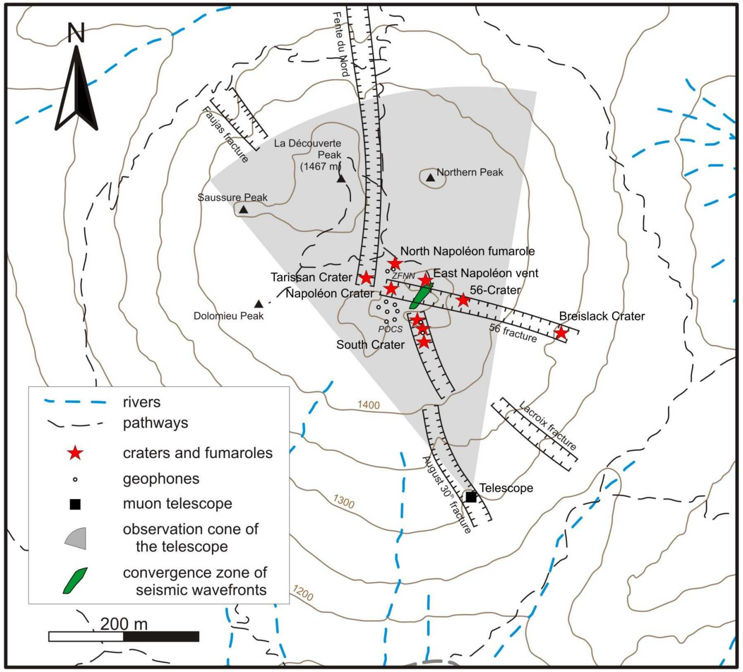

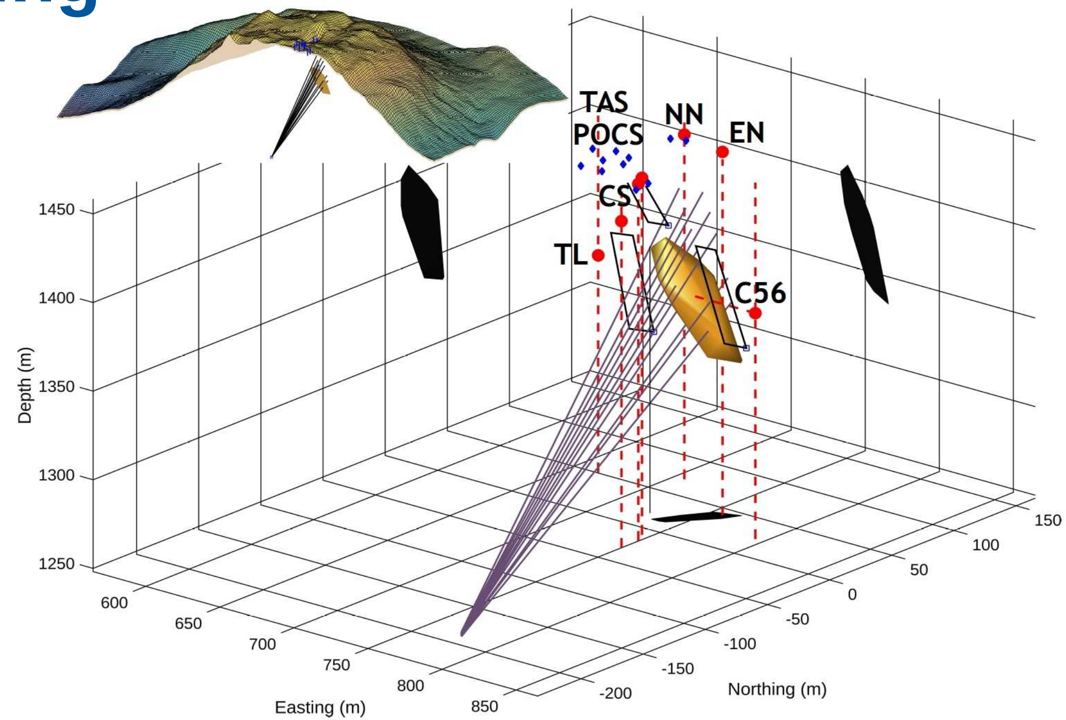

Global analysis of muon and seismic monitoring

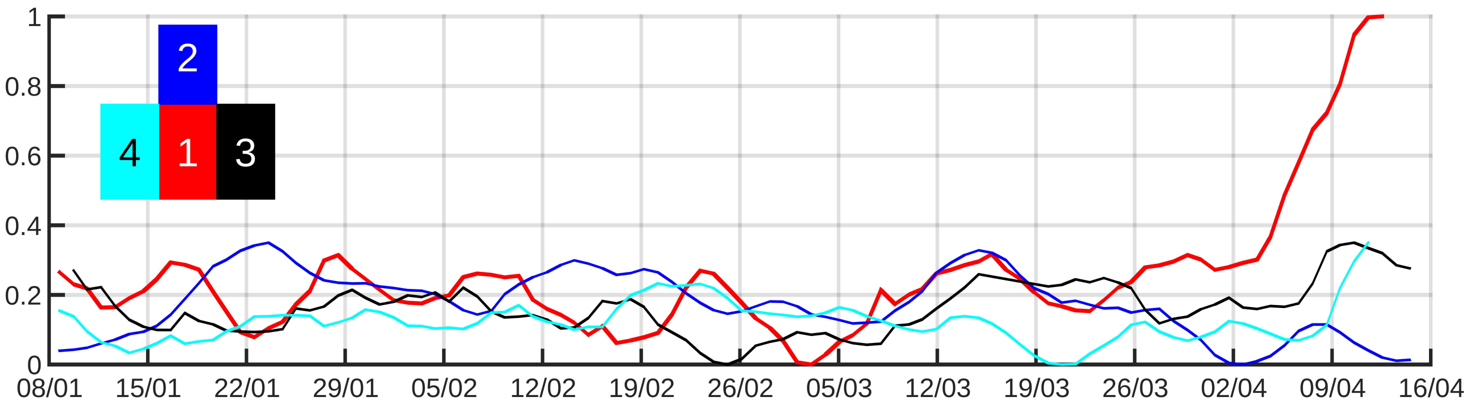

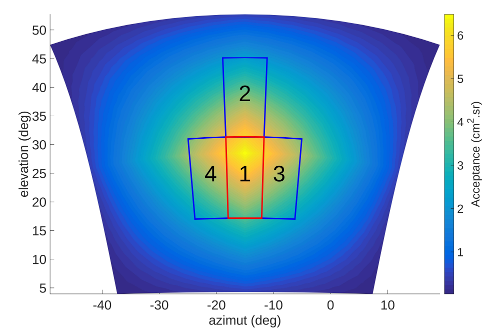

Abrupt changes of hydrothermal activity in a lava dome detected by combined seismic and muon monitoring : *Le Gonidec, J.-Y. et al. Scientific Reports 2019*

Snaefellsjökull 2nd run

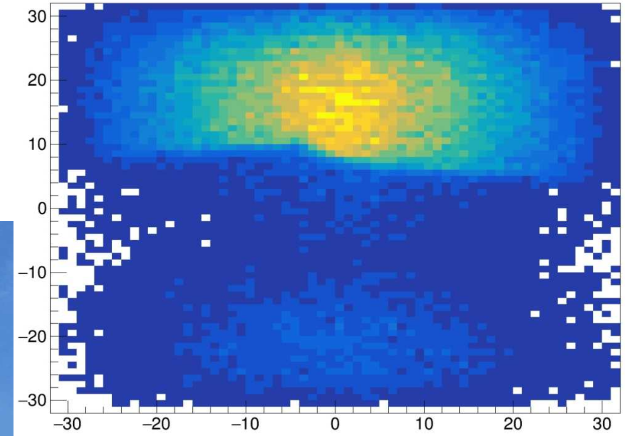

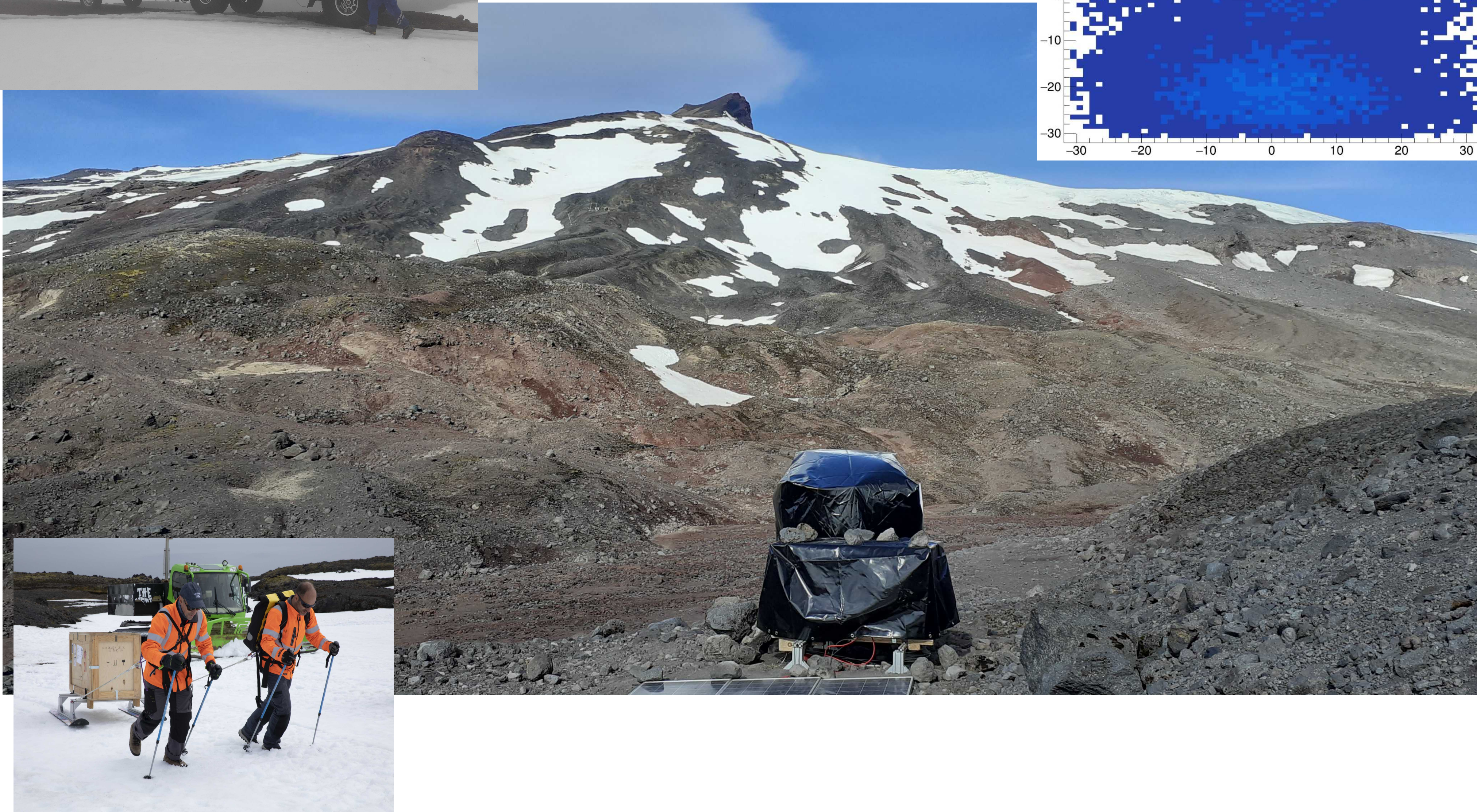

Nuclear evaporator

TBM

MUODIM

Silos

Geotechnics

Blast furnace

Glass furnace

Application to Blast Furnaces

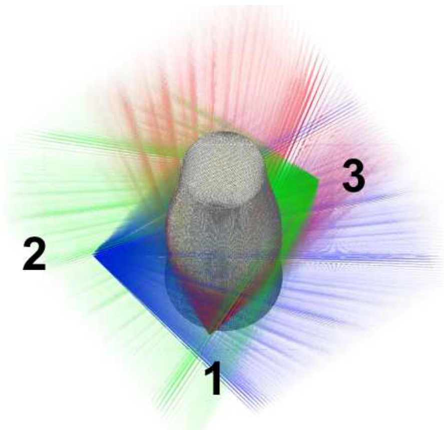

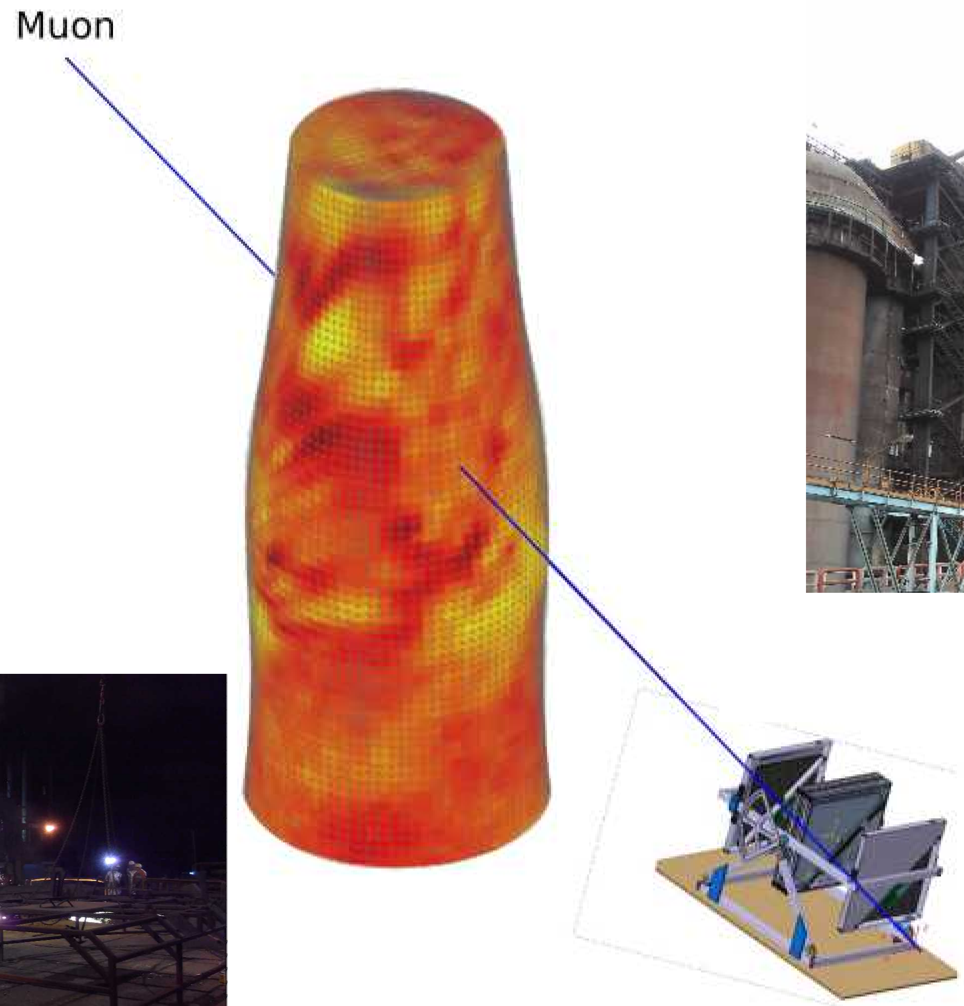

https://arxiv.org/abs/2301.04354

Confidentiel

Application to Tunnel Boring machines

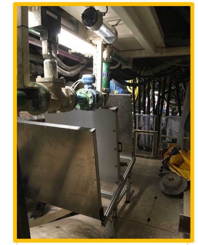

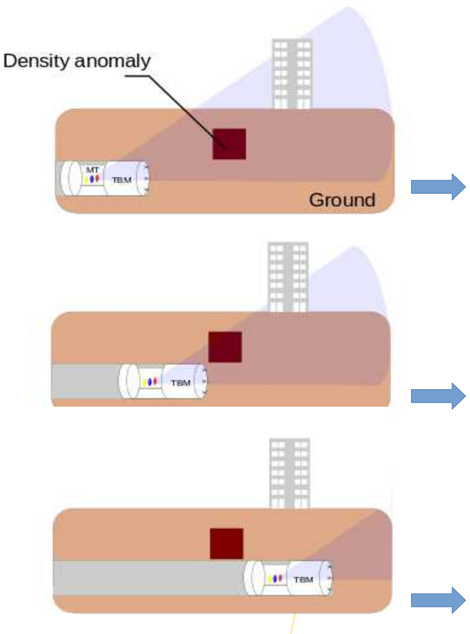

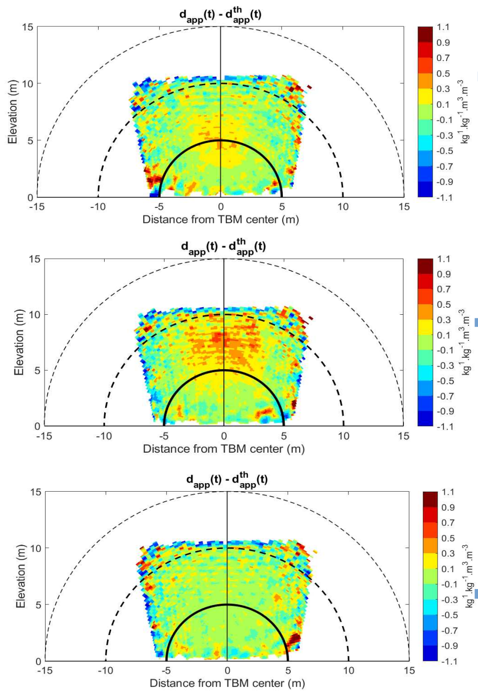

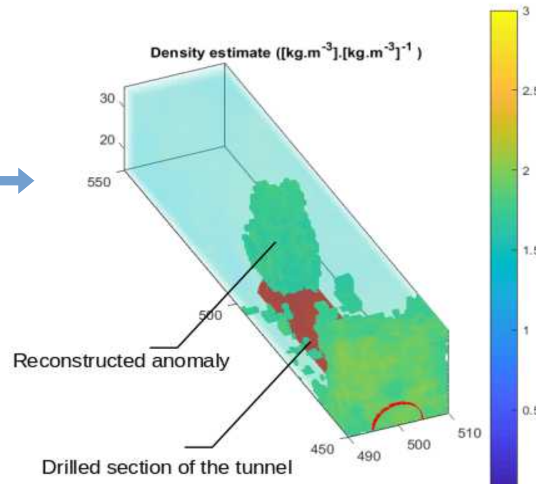

Archaeology

Great pyramids

Search for Hidden Chambers in the Pyramids

The structure of the Second Pyramid of Giza is determined by cosmic-ray absorption.

Luis W. Alvarez, Jared A. Anderson, F. El Bedwei, James Burkhard, Ahmed Fakhry, Adib Girgis, Amr Goneid, Fikhry Hassan, Dennis Iverson, Gerald Lynch, Zenab Miligy, Ali Hilmy Moussa, Mohammed-Sharkawi, Lauren Yazolino

Palais du miroir :

- *georadar + ERT*
- *DAS (optical fiber seismology)*
- *muography*

Apollonia

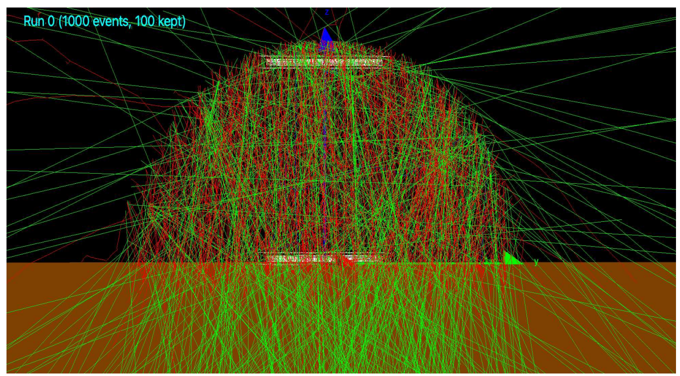

Palais du miroir

Overburden Thickness Calculation

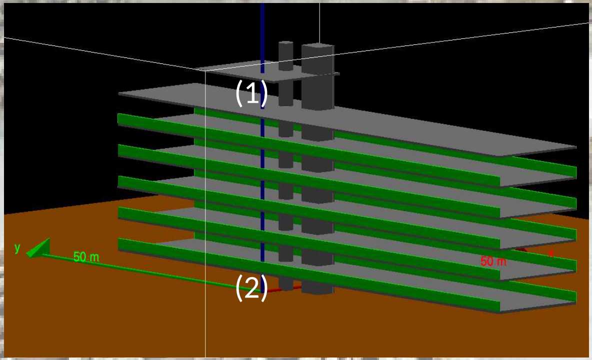

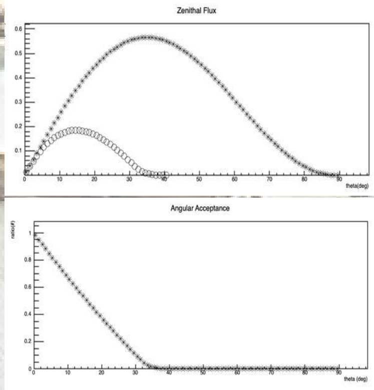

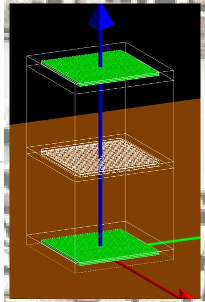

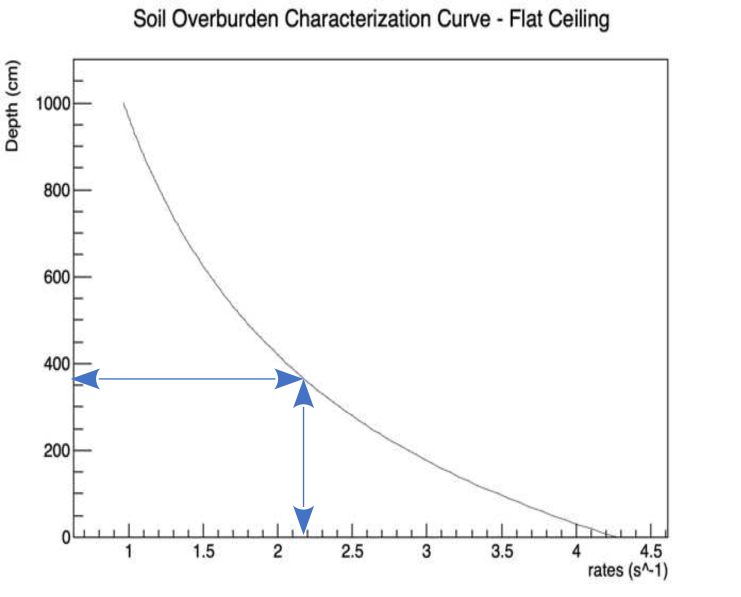

<u>Detector Efficiency Calculation</u>

Theoretical Rates:

(1) - 4.120 s^-1

(2) - 3.175 s^-1

Experimental Rates:

(1) – 0.637 ± 0.0021 s^-1

(2) – 0.480 ± 0.0027 s^-1

Efficiency:

(3) - 0.1546 ± 0.0005

(4) - 0.1512 ± 0.0009

<Efficiency>: 0.1524 ± 0.0004

<u>Experimental rate inside the Cavity</u>

1st Run: 0.3381 ± 0.0007 s^-1

2nd Run: 0.3384 ± 0.0009 s^-1

3rd Run: 0.3209 ± 0.0008 s^-1

<Rate> = 0.3326 ± 0.0005 s^-1

Divide by efficiency

Rate = 2.182 ± 0.003 s^-1

<u>Overburden Characterization Curves</u>

Two Geometries for the overburden.

(a) Rectangular &

(b) Rectangular with Semispherical Cavity

The material is Standard Rock

The step for the curve points is 10 cm

Height (a) = 362.9 ± 0.9 cm

Height (b) = 358.4 ± 0.9 cm

<Height> = 360.7 ± 0.6 cm

GeoRadar & ERT & Distributed Acoustic Sensing & Seismometry

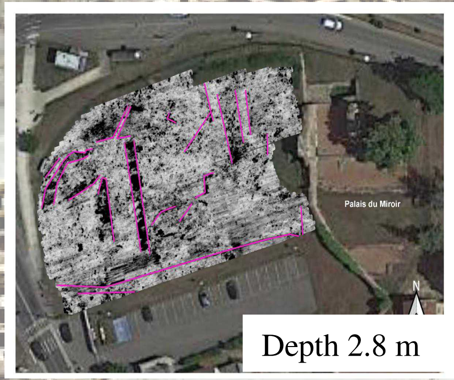

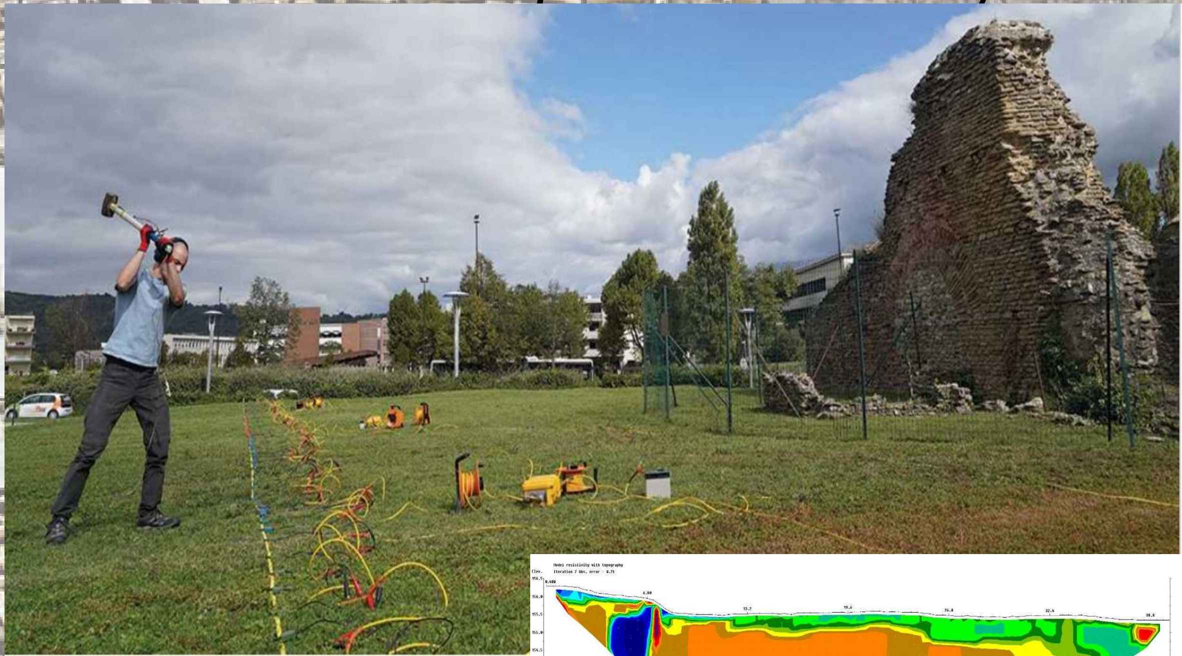

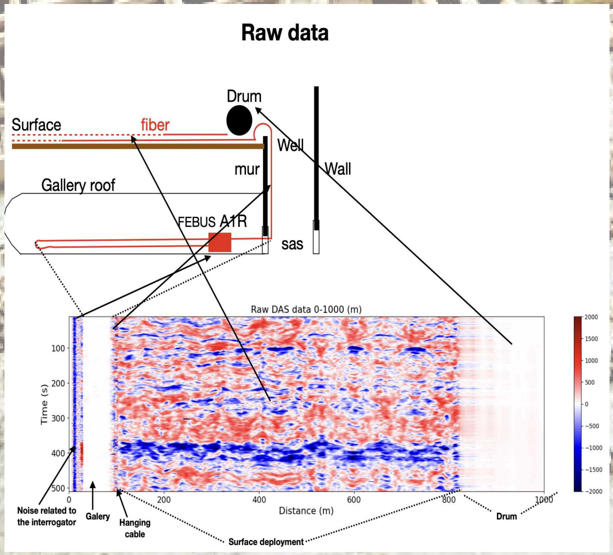

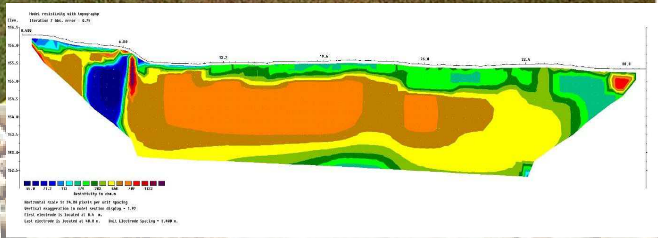

Atmospheric & hydrogeological effects

How soil water retention affects the measurement

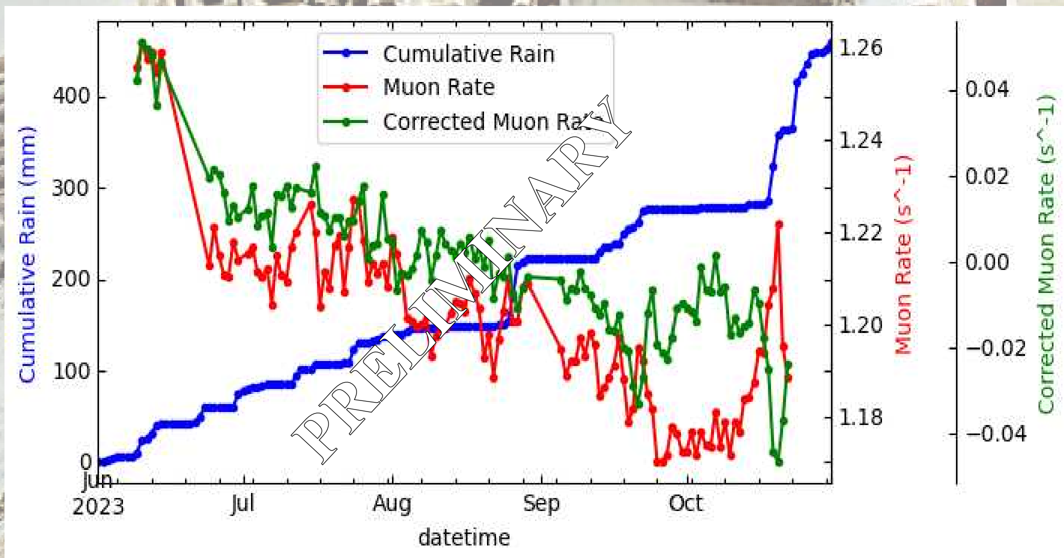

$$\frac{\Delta R}{\langle R\rangle} = \alpha_T \frac{\Delta T_{\text{eff}}}{\langle T_{\text{eff}}\rangle} + \beta_P (p - \langle p\rangle)$$

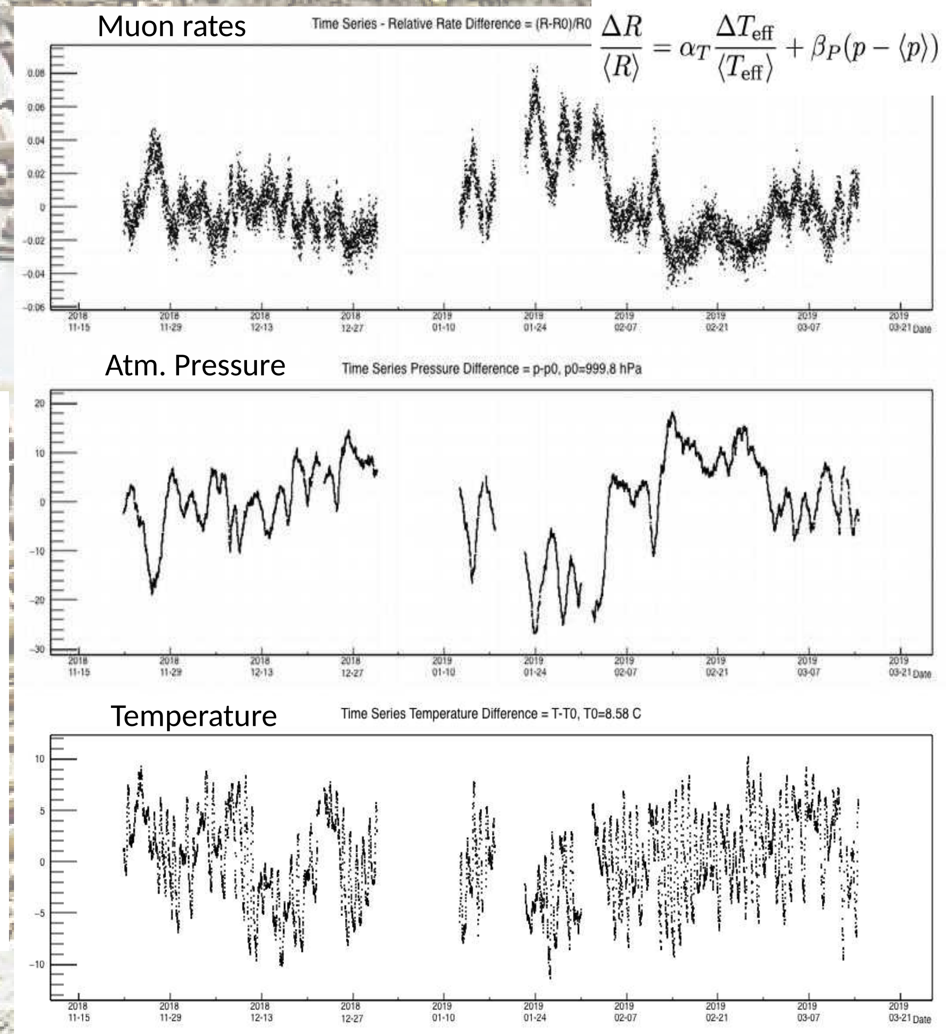

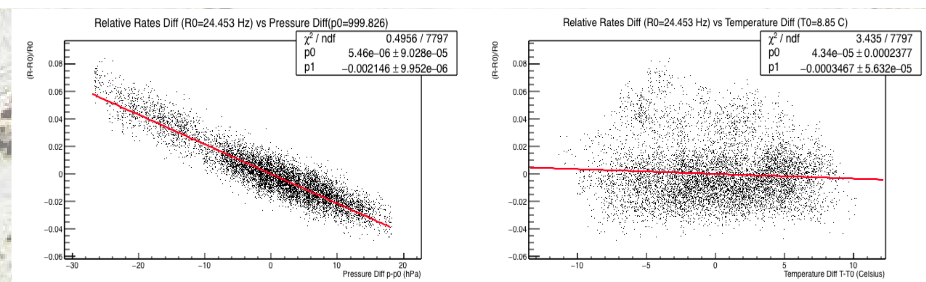

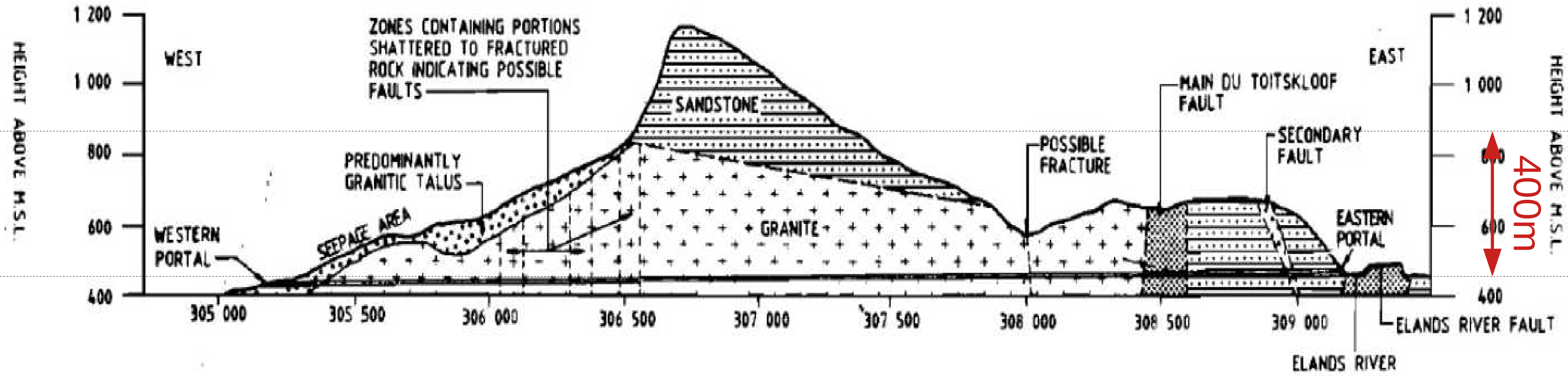

From Mont-Terri to PAUL

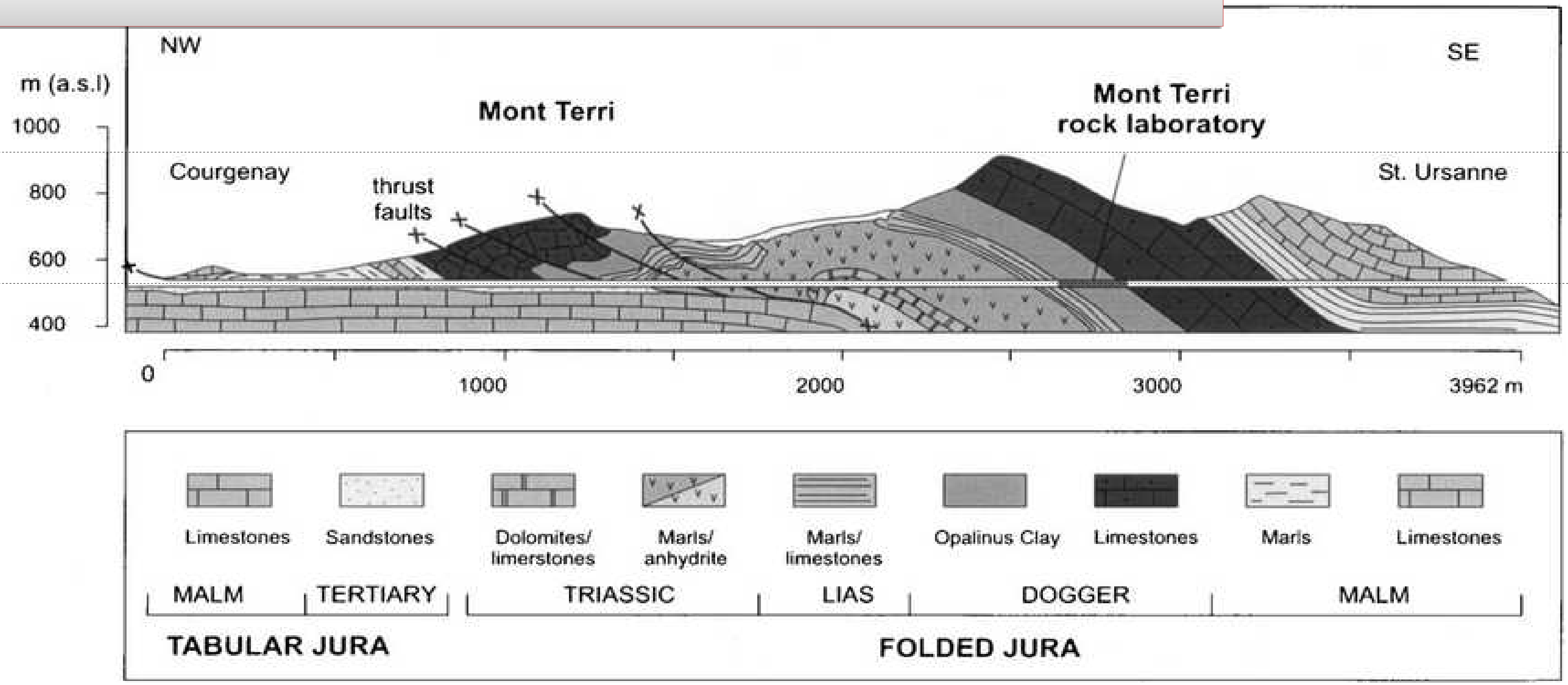

Muography underground : Mont-Terri (Switzerland), Tournemire, LSBB + urban tunnels (France)

(-400m) (-200-250m) (-30-500m) (-10-50m)

LSBB
Laboratoire Souterrain à Bas Bruit
Low Noise Inter Disciplinary Underground Science & Technology

A GOOD EXAMPLE: THE BUISSONIÈRE EXPERIMENT

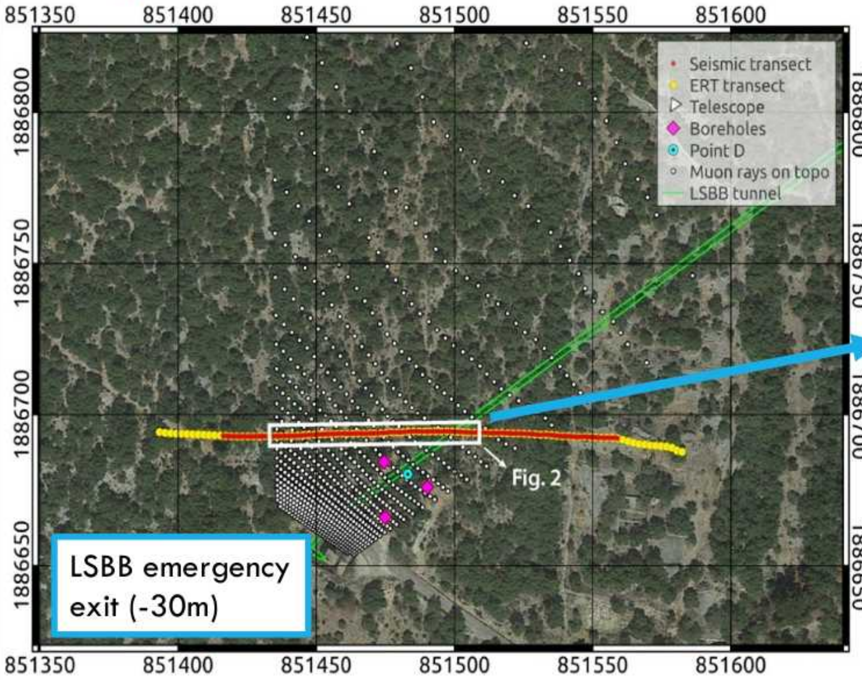

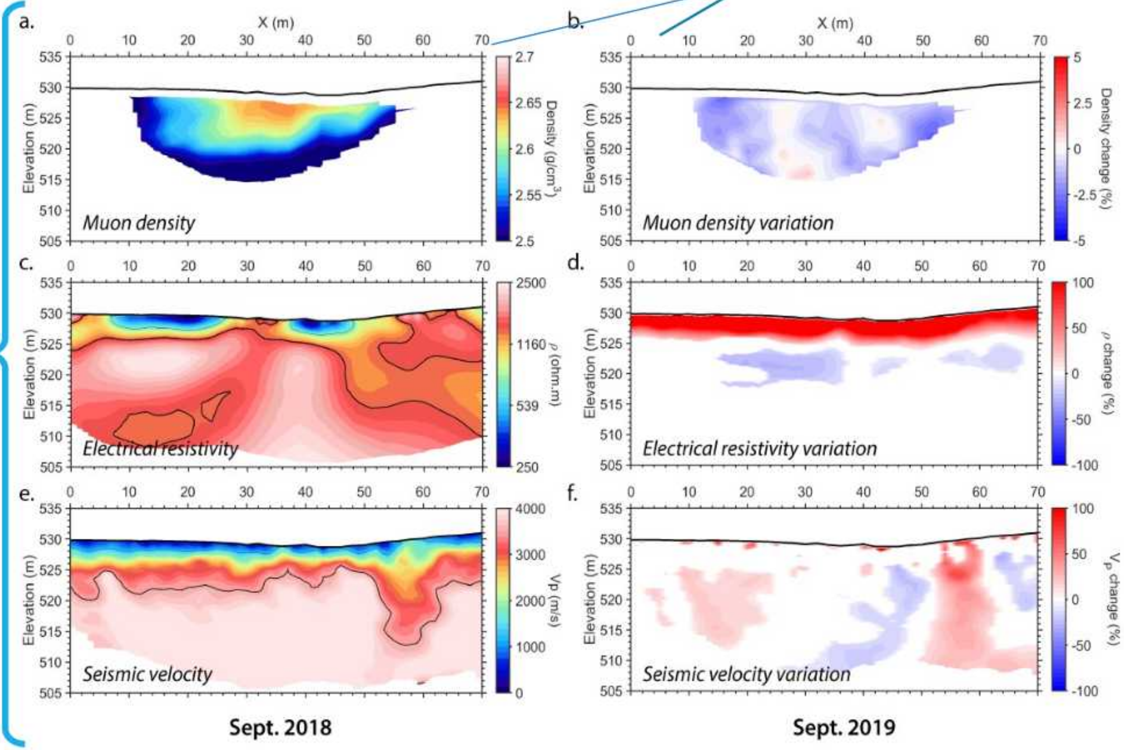

Ref: Lázaro Roche, I.; Pasquet, S.; Chalikakis, K.; Mazzilli, N.; Rosas-Carbajal, M.; Decitre, J.B.; Batiot-Guilhe, C.; Emblanch, C.; Marteau, J.; et al.
Water resource management: The multi-technique approach of the Low Background Noise Underground Research Laboratory of Rustrel, France, and its muon detection projects.
In Muography: Exploring Earth's Subsurface with Elementary Particles. **2021**, Geophysical Monograph Series; Oláh, L., Tanaka, H., Varga, D., Eds. American Geophysical Union , USA. DOI:10.1002/9781119722748.ch10

Context : the Huguenot tunnel & the PAUL project

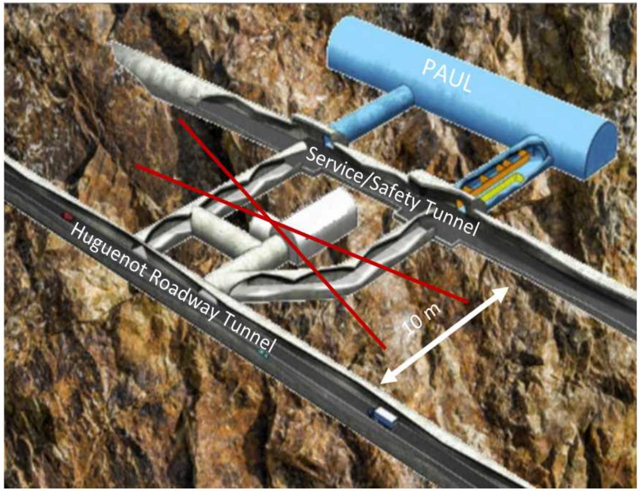

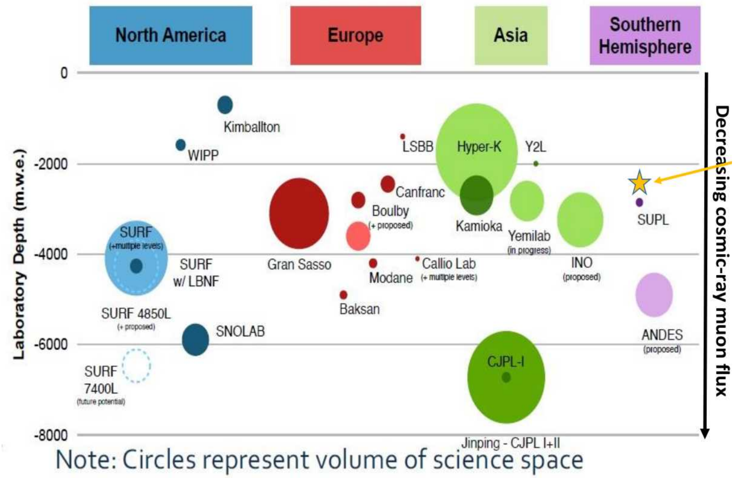

Challenge : qualifying the rock overburden

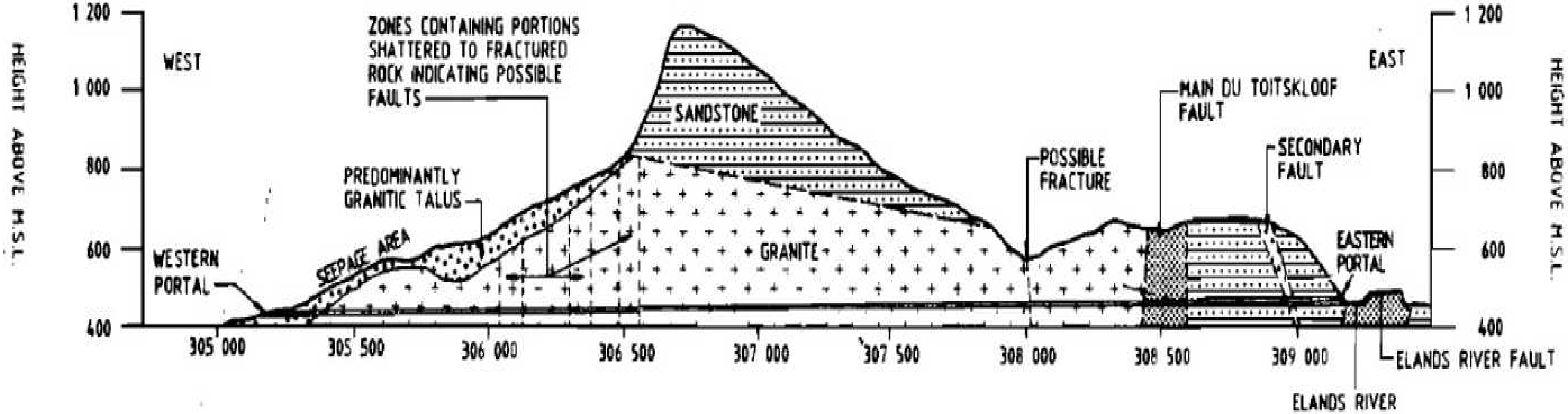

2008-2011 : *N.Lesparre thesis*

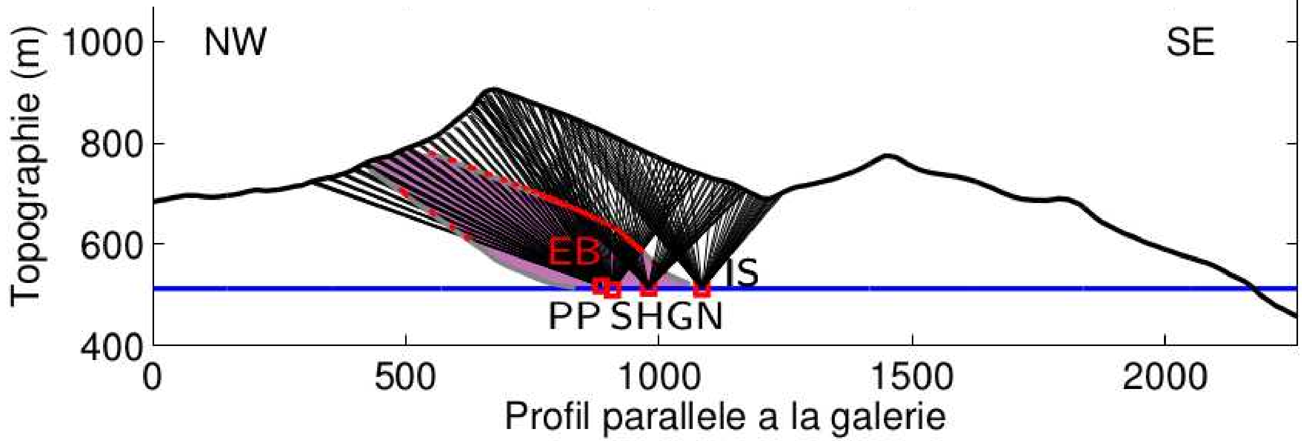

Bruit de fond décorrélé dans la niche PP : 1.7×10^{-7}/s

EB (177 jours)

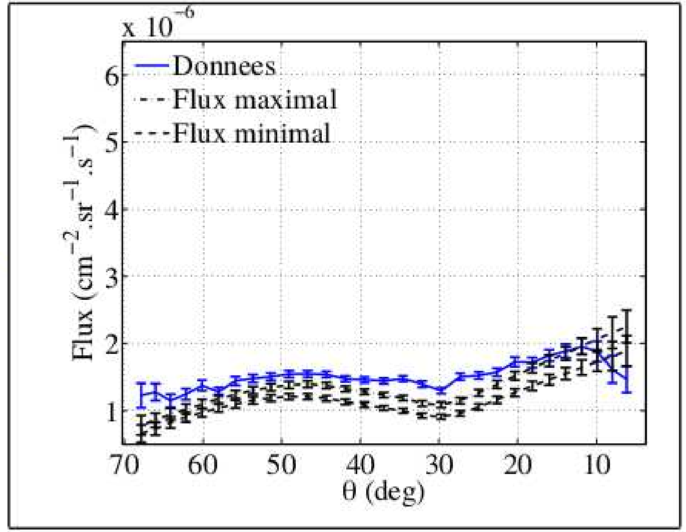

PP (56 jours)

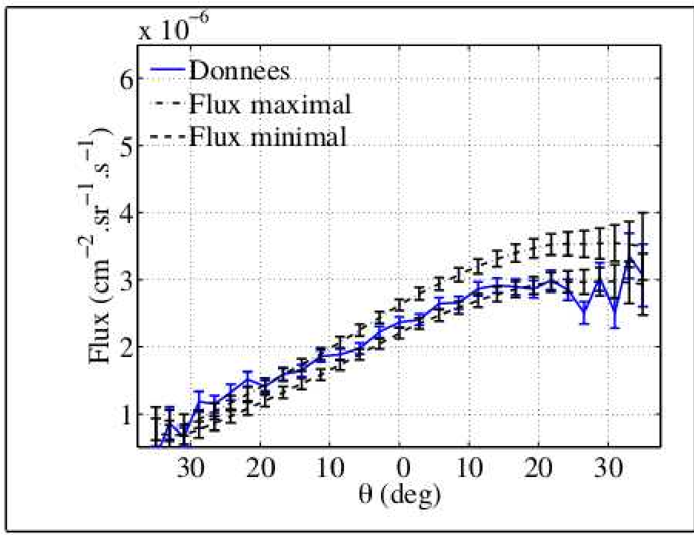

SHGN (42 jours)

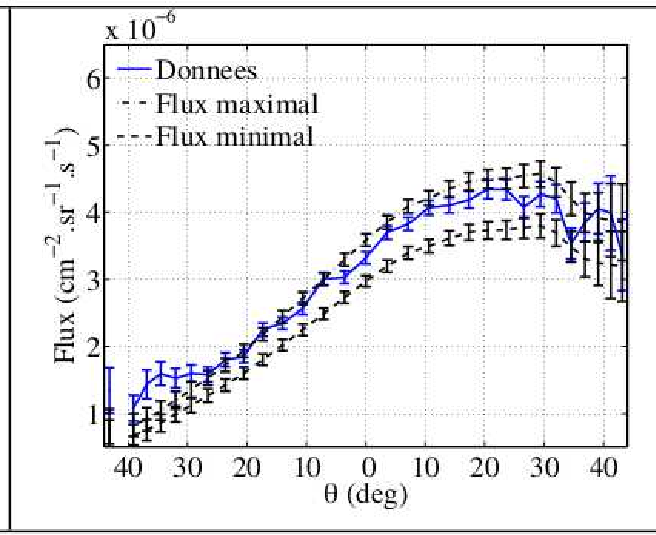

IS (47 jours)

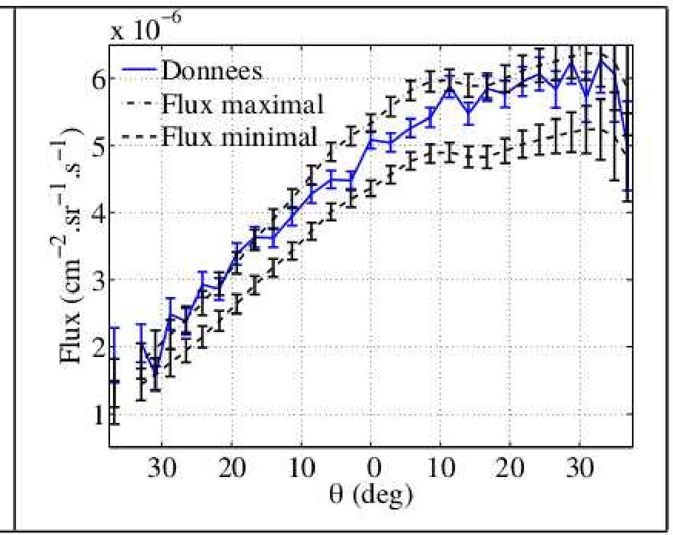

2012-2015 : *K.Jourde thesis*

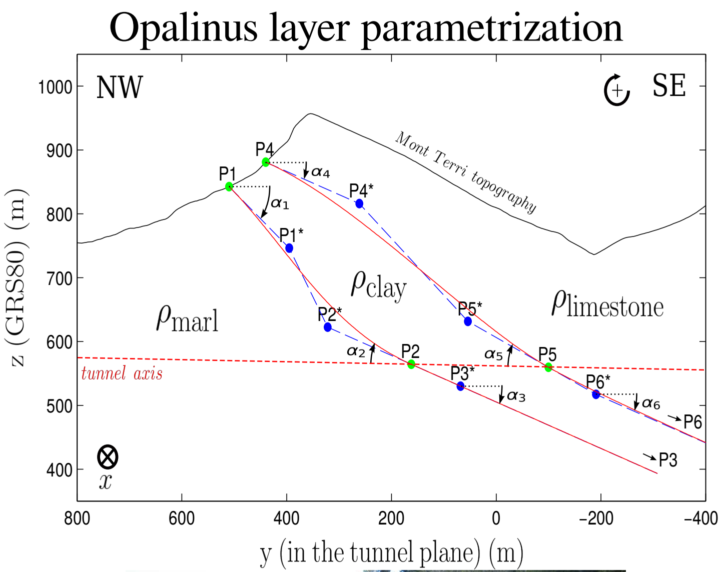

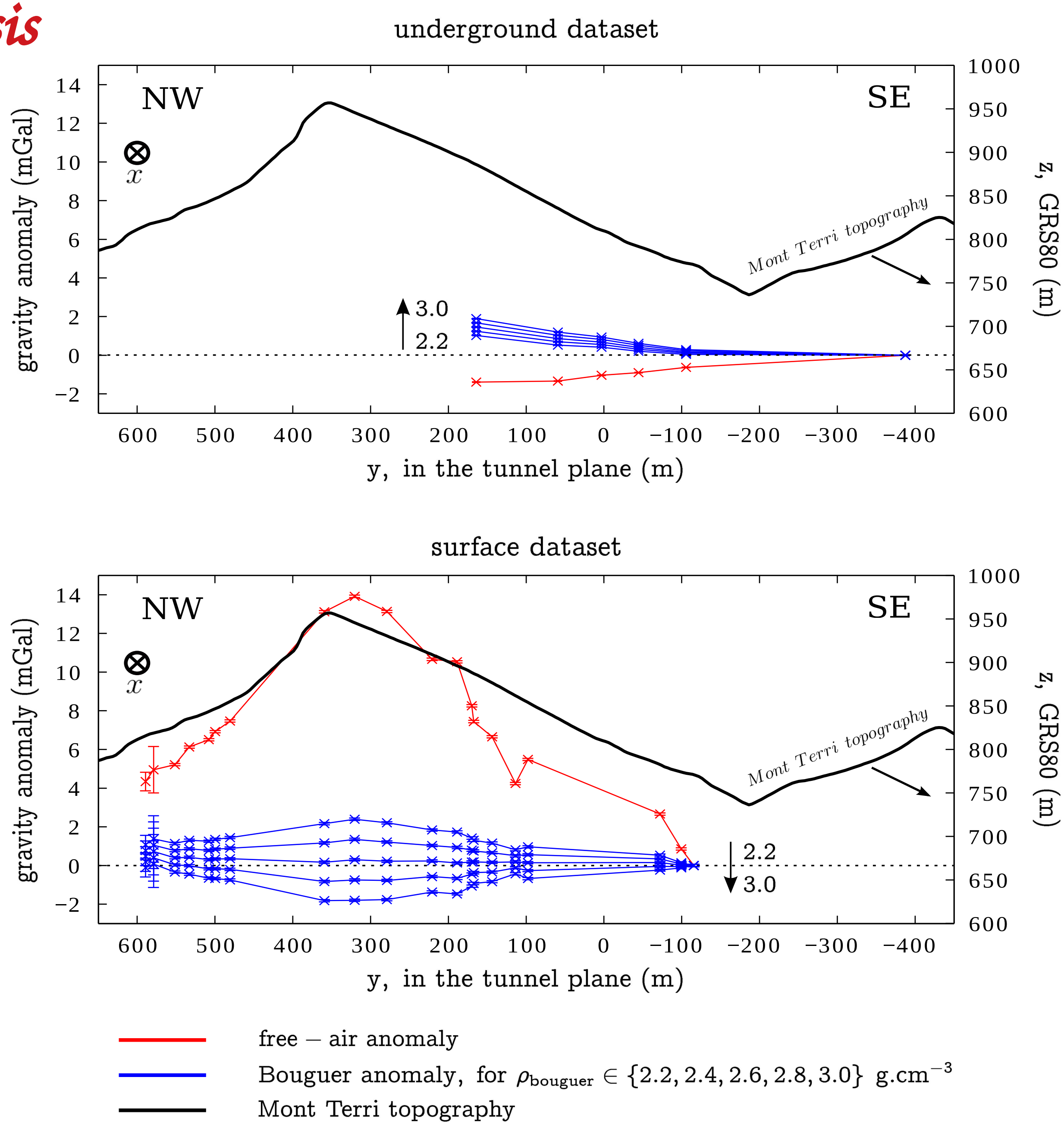

2012-2015 : *K.Jourde thesis*

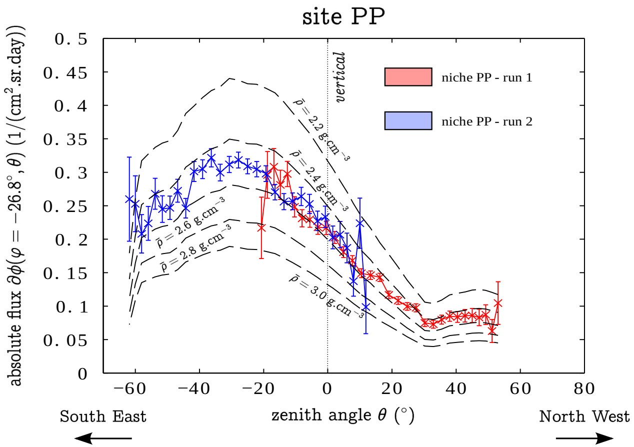

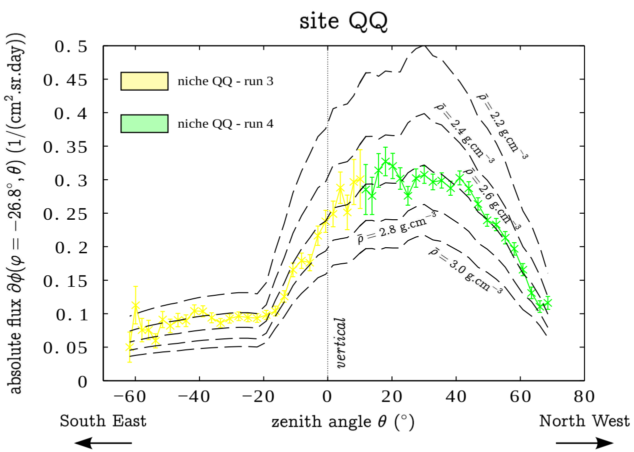

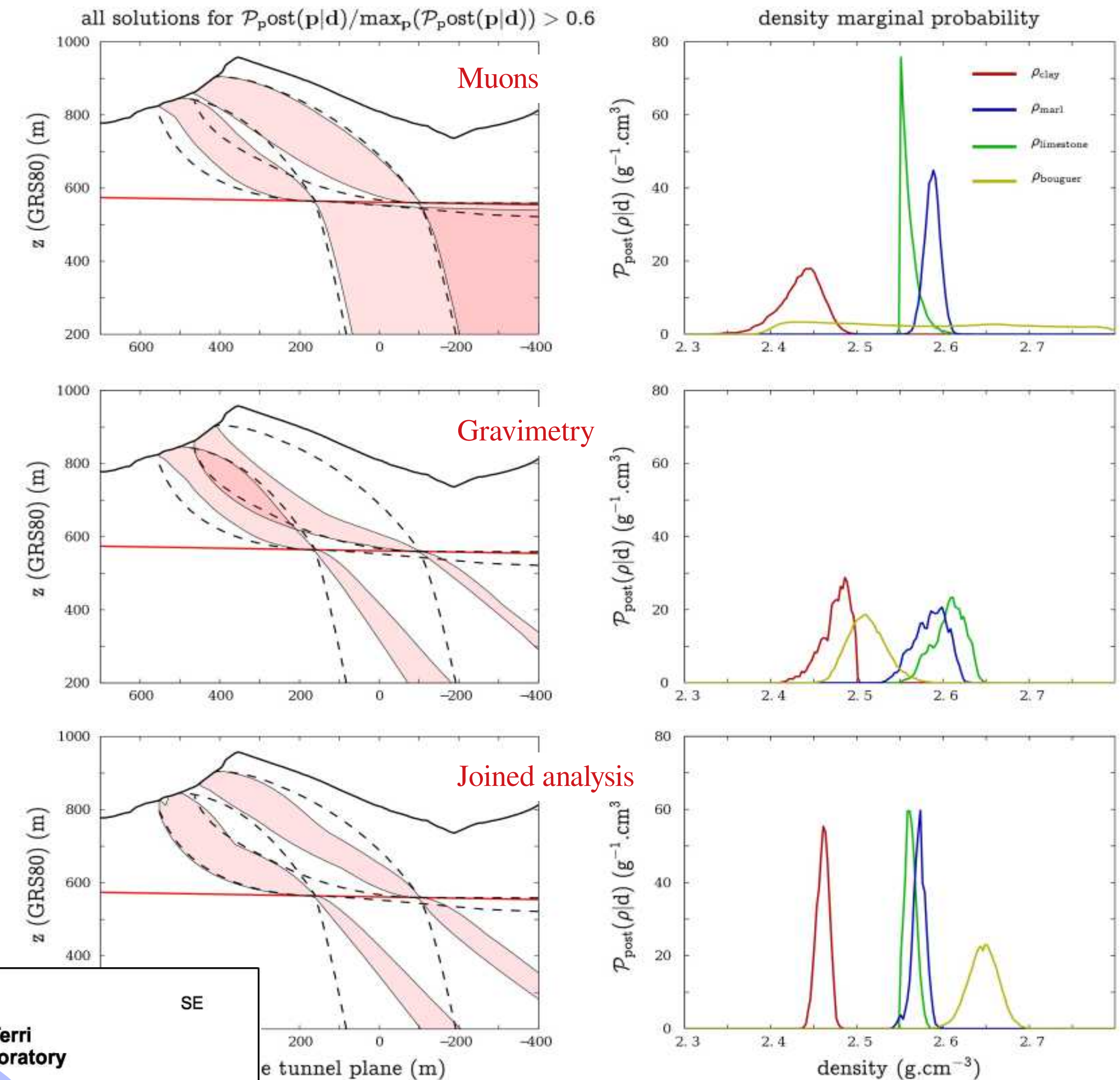

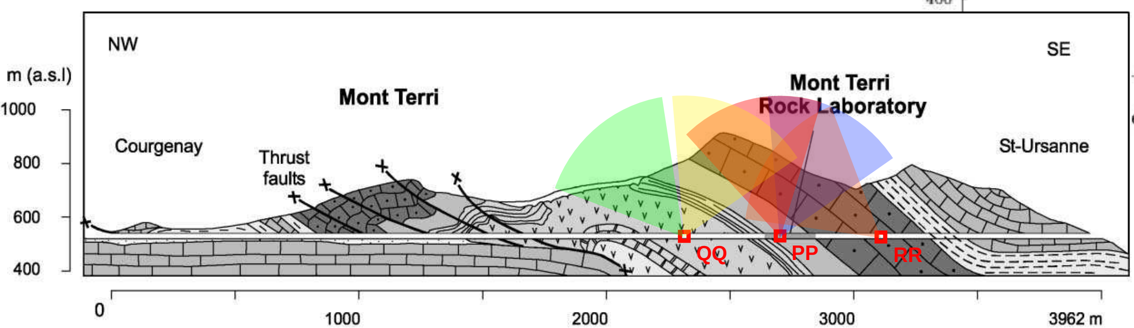

2016-2018 : *karstic system monitoring + SSW observations*

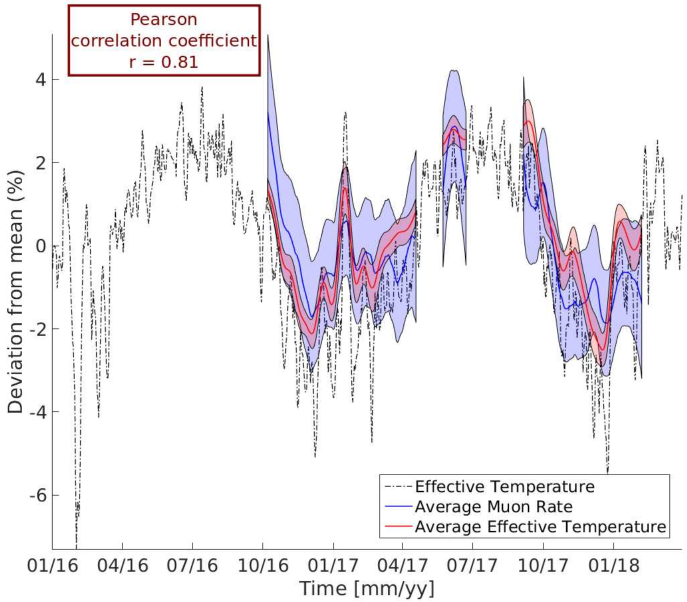

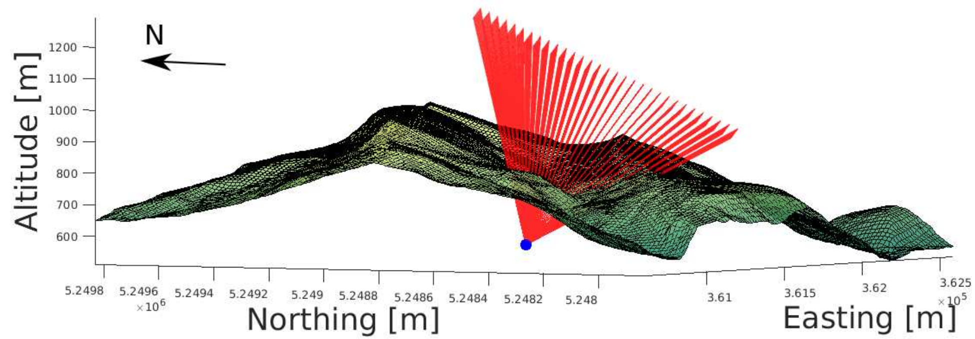

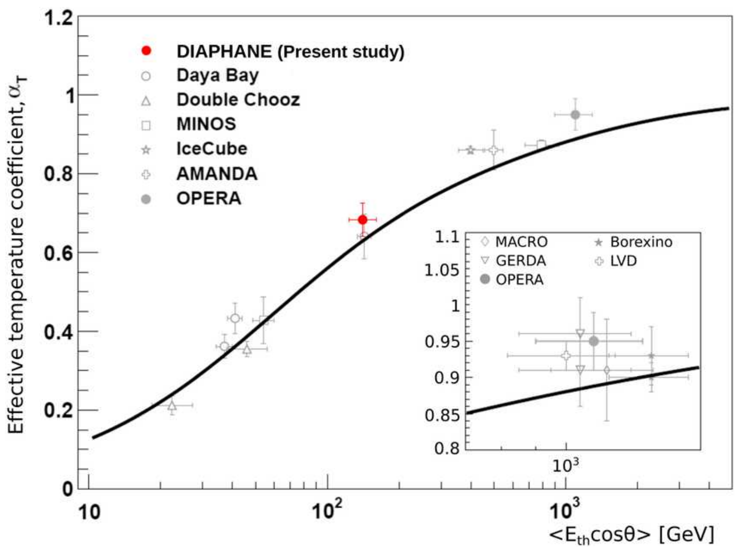

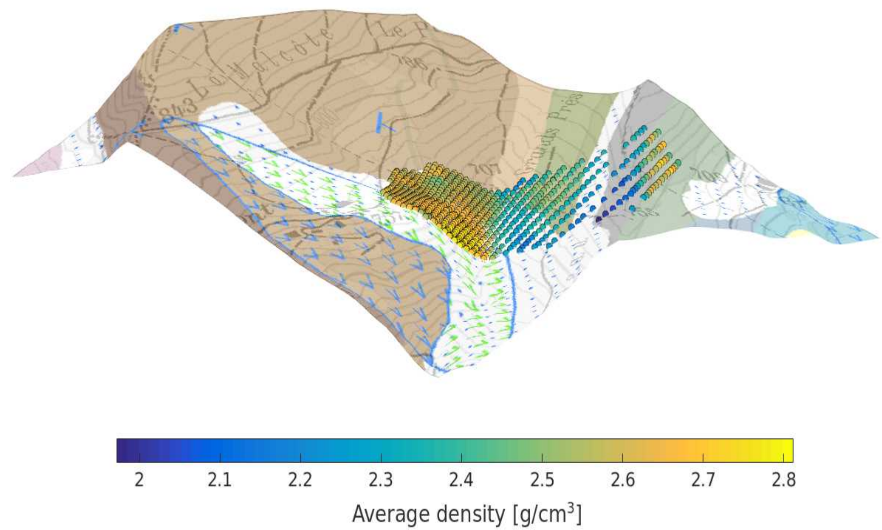

Atmospheric physics + hydro-geological measurements

SSW physics

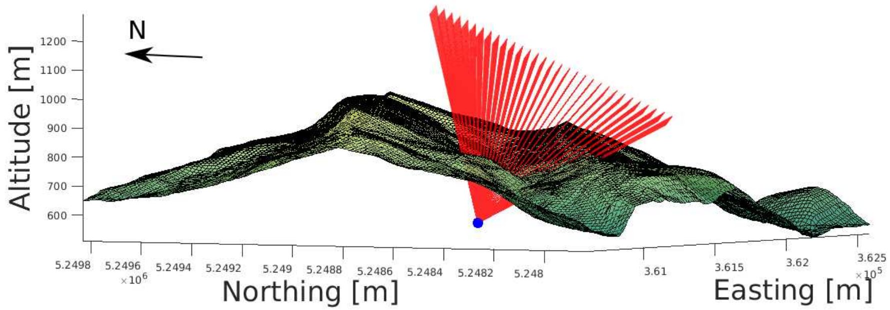

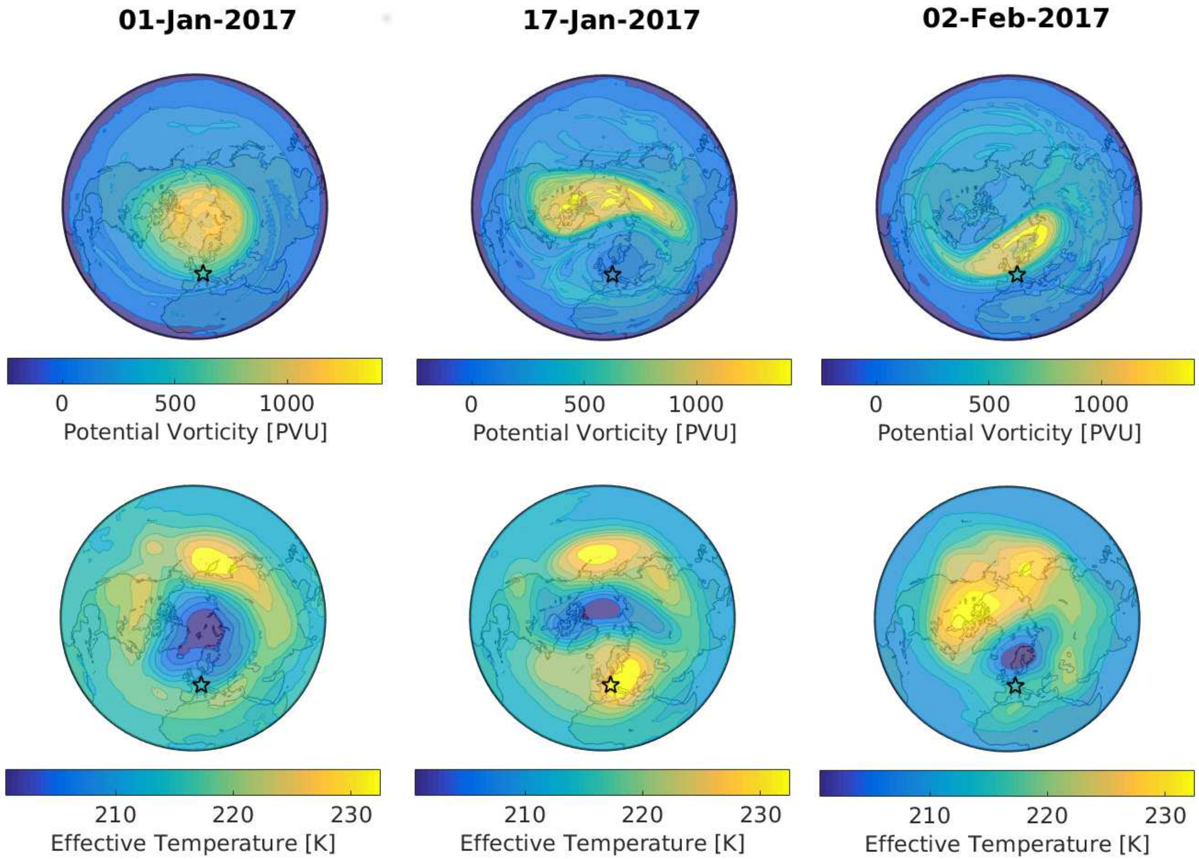

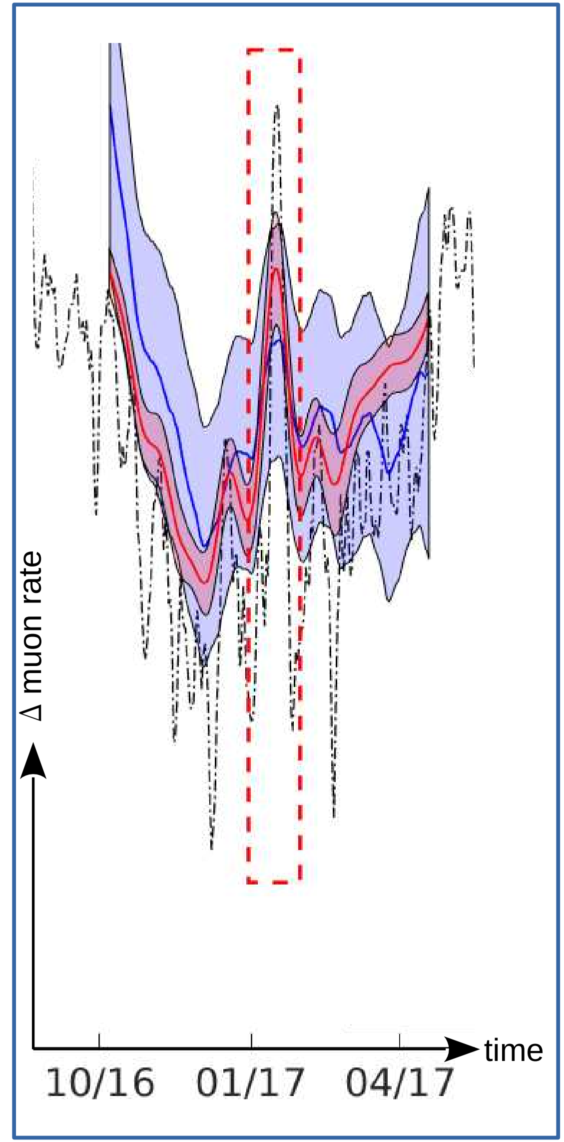

Tramontini, M. & Rosas-Carbajal, M. & Nussbaum, C. & Gibert, D. & Marteau, J.. (2019). Middle-Atmosphere Dynamics Observed With a Portable Muon Detector. Earth and Space Science. 6. 10.1029/2019EA000655.

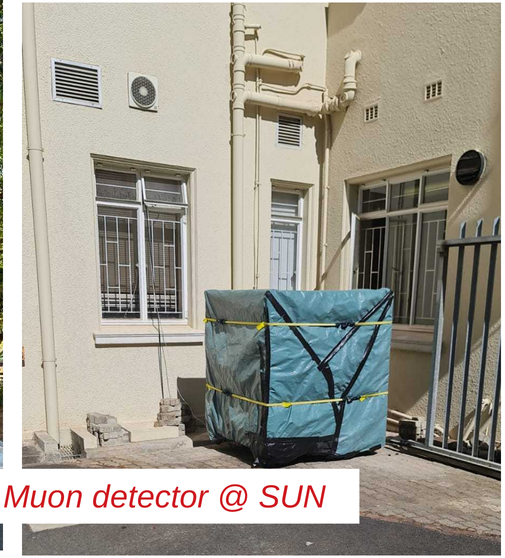

Muon detector @ SUN

Muon detector @ SUN

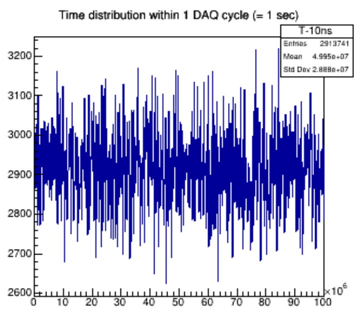

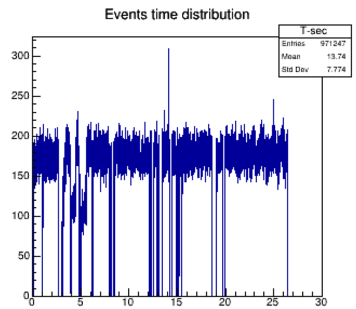

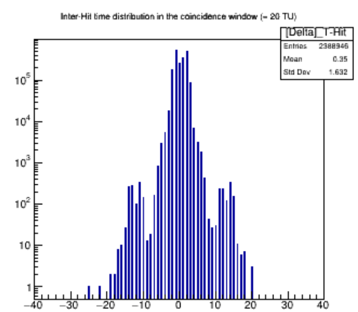

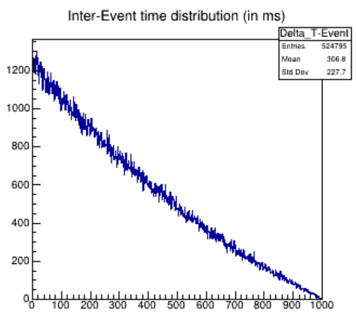

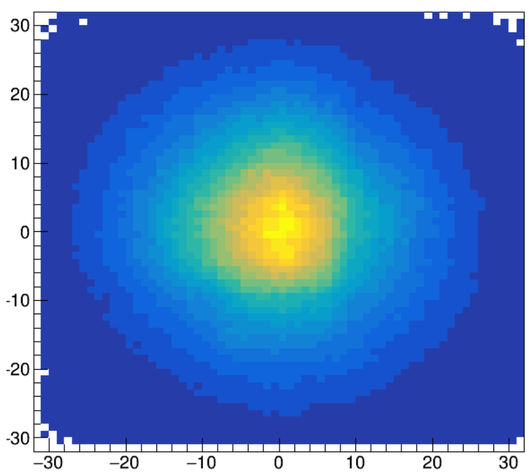

Muon detector ready @IP2I

Muography @PAUL

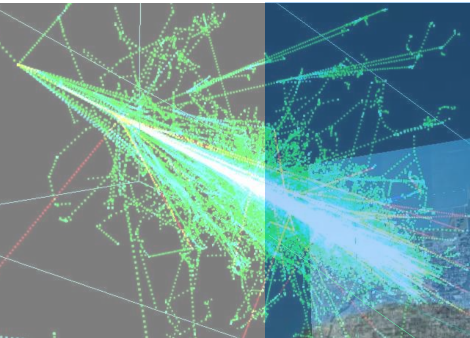

Stay tuned !